

Novel Core-Expanded Perylene Diimide Dye: Synthesis, Characterization and Optical Properties

Adamu Abubakar

Submitted to the
Institute of Graduate Studies and Research
in partial fulfillment of the requirements for the degree of

Master of Science
in
Chemistry

Eastern Mediterranean University
July 2016
Gazimağusa, North Cyprus

Approval of the Institute of Graduate Studies and Research

Prof. Dr. Cem Tanova
Acting Director

I certify that this thesis satisfies the requirements as a thesis for the degree of Master of Science in Chemistry.

Prof. Dr. Mustafa Halilsoy
Chair, Department of Chemistry

We certify that we have read this thesis and that in our opinion it is fully adequate in scope and quality as a thesis for the degree of Master of Science in Chemistry.

Prof. Dr. Huriye İcil
Supervisor

Examining Committee

1. Prof. Dr. Huriye İcil

2. Asst. Prof. Dr. Süleyman Aşır

3. Asst. Prof. Dr. Nur P. Aydinlik

ABSTRACT

Perylene molecules bearing two aryloxy substituents on bay position (1,7 positions) and two receptor units at the imide positions are most useful fluorescent building blocks for the realization of a broad variety of self-assembly architectures. High absorption of perylene diimides (PDIs) in the visible region offers many advantages for photonic applications, optimum electron transport properties, flexible synthetic potentials to adjust energy levels, solubility, stacking properties, excellent thermal and photo-stability.

In this thesis, a novel perylene diimide with tyramine substitution at the bay (1,7-position) and imide position was designed and synthesized successfully. The synthesized product was characterized by FTIR, UV-vis, emission, TGA, DSC techniques and elemental analysis. The photophysical and thermal properties of Ty-B-PDI reveal that it as a good candidate for photovoltaic applications.

Keywords: perylene diimides, Tyramine, electron transport, Self-assembly.

ÖZ

Körfez-süstitüe perilen diimidler, kendiliğinden düzenleme yapabilen yapılarda kullanıma çok uygun floresans yapı taşlarıdır. Görünür bölgede güçlü absorblama yapan perilen diimidlerin fotonik uygulamalarda en önemli avantajları; optimum elektron taşıma özellikleri, enerji seviyesi değışebilir sentez esnekliğı, çözünlük, yığılaşma özellikleri, mükemmel termal ve foto kararlılıklarıdır.

Bu tezde, gerek körfez (1,7 pozisyonları) ve gerekse imid pozisyonlarında tiraminin süstitüe olduğı çok yeni bir perilen diimid başarıyla sentezlenmiştir (Ty-B-PDI). Bu bileşik, FT-IR, UV-görünür, emisyon, elemental analiz, TGA ve DSC teknikleriyle ayrıntılı bir şekilde karakterize edilmiştir. Fotofiziksel ve termal özellikler , Ty-B-PDI diimidin fotovoltaiik uygulamalar için çok uygun aday bir pigment olduğunu göstermektedir.

Anahtar Kelimeler: perilen diimidlerin, elektron taşıma, tiraminin, kolayca kurululabilirlik

To My Family

ACKNOWLEDGEMENT

I give thanks to the Almighty Allah, on whom we completely count for guidance and sustenance.

Immeasurable appreciation and sincere gratitude goes to my esteem research supervisor, **Prof. Dr.Huriye Icil**, for giving me the opportunity to carry out the research under her supervision and guidance. Her determination, vision, honesty, motivation and empathy have deeply inspired me. It was indeed a great privilege and honor to work under her guidance. I am extremely grateful ma'am.

My special thanks go to, Basma Basil Ismael Al-khateep, who has been always there to listening and give practical advice. Am deeply grateful to her for the lab work and long discussion that assisted me to type out the technical detail of my thesis.

I am also indebted to members of the İcil organic research group family with whom I have interacted during the course of my graduate studies. Particularly, I would like to acknowledge Dr. Duygu Uzun, Melika Mostafanejad, Karar Shukur, Maryam Pakseresht, Melten Dinleyeci, Courage Akpan, Sümeyye Kırkinci Yılmaz, Hengame Jowzaghi and Selin Temürlü. I greatly value you and deeply appreciate for your kind support.

Most essentially, none of this would have been possible without the support, love and patient of my family especially my closed family for whom this thesis is dedicated to. I can find words to express my utmost gratitude to you but to continuous praying for you for the rest of my life.

TABLE OF CONTENTS

ABSTRACT	iii
ÖZ	iv
LIST OF TABLES	ix
LIST OF FIGURES	x
LIST OF SCHEMES	xii
LIST OF SYMBOLS/ABBREVIATION	xiii
1 INTRODUCTION	1
1.1 Perylene Dyes	1
1.2 Bay Substituted Perylene Diimide	3
1.3 Electron Transport Properties of Bay Substituted Perylene Diimide	5
2 THEREOTICAL	7
2.1 Synthesis and Applications of Perylene Dye	7
2.2 Synthesis and Applications of Bay Substituted Perylene Diimides	9
2.3 Electron Transfer	11
2.4 Organic Solar Cells and Their Applications	13
3 EXPERIMENTAL	17
3.1 Materials	17
3.2 Instruments	17
3.3 Method of Synthesis	17
3.4 General Synthesis of Ty-B-PDI	18
3.5 Synthesis of Ty-B-PDI	20
3.6 General Reaction Mechanism of Perylene Diimide	22
4 DATA AND CALCULATION	24

4.1 Optical and Photochemical Properties	24
5 RESULTS AND DISCUSSION	52
5.1 Synthesis and Characterization	52
5.2 Absorption and Fluorescence Properties	54
5.3 Mass Spectra Analysis.....	56
5.4 Thermal Stability	56
CONCLUSION.....	57
REFERENCES	59
Appendix A: Curriculum Vitae.....	68

LIST OF TABLES

Table 4.1.1: Molar absorption coefficients of Ty-B_PDI in different solvents.....	25
Table 4.1.2: Fluorescence quantum yield of Ty-B-PDI	27
Table 4.1.3: Half-width of the selected maximum Absorption of Ty-B-PDI.....	29
Table 4.1.4: Theoretical radiative lifetime of Ty-B-PDI in different solvents.....	30
Table 4.1.5: Theoretical fluorescence lifetime of Ty-B-PDI....	31
Table 4.1.6: Fluorescence Rate Constants data of Ty-B-PDI.....	32
Table 4.1.7: Rate constants of radiationless Deactivation	32
Table 4.1.8: Oscillator strengths data of Ty-B-PDI.....	33
Table 4.1.9: Singlet energies data of Ty-B-PDI	34
Table 5.1: The solubility properties of Ty-B-PDI in different solvents ...	34

LIST OF FIGURES

Figure 1.1: A General structure of Perylene, PDA and PDI	1
Figure 1.2: Structures of different colored PDIs pigments	2
Figure 1.3: The chemical structure of brominated PDA and PDI derivatives	4
Figure 1.4: Structural representation of bay and Immidization position of Ty-B-PDI	6
Figure 1.5: 3-D structural representation of bay and Immidization position of Ty-B-PDI	6
Figure 2.1: Electron transfer between Donor and Acceptor	12
Figure 2.2: the devices system of a) bilayer heterojunction, b) bulk heterojunction, c) working principle of the device	15
Figure 4.1: Representative spectra of Half-width with the selected Absorption	28
Figure 4.2: FT-IR Spectrum of Tyramine	35
Figure 4.3: FT-IR Spectrum of Br-PDA	36
Figure 4.4: FT-IR spectrum of Ty-B-PDI	37
Figure 4.5: Absorbance spectrum of Ty-B-PDI in DMF	38
Figure 4.6: Absorption spectrum of Ty-B-PDI in DMF after microfiltration	39
Figure 4.7: Absorption spectrum of Ty-B-PDI in NMP	40
Figure 4.8: Absorption spectrum of Ty-B-PDI in NMP after microfiltration	41
Figure 4.9: Absorption spectrum of PDI-Tyra in TFA	42
Figure 4.10: Absorption spectrum of Ty-B-PDI in DMF, NMP and TFA	43
Figure 4.11: Emission spectrum of Ty-B-PDI in DMF	44
Figure 4.12: Emission spectrum of Ty-B-PDI in DMF after microfiltration	45
Figure 4.13: Emission spectrum of Ty-B-PDI in NMP	46
Figure 4.14: Emission spectrum of Ty-B-PDI in NMP after microfiltration	47

Figure 4.15: Emission spectrum of Ty-B-PDI in TFA	48
Figure 4.16: Emission spectrum of Ty-B-PDI in DMF, NMP and TFA	49
Figure 4.17: DSC Curve of Ty-B-PDI at the heating $10^0\text{C}/\text{min}$ in nitrogen	50
Figure 4.18: TGA thermogram of Ty-B-PDI at heating rate of $10^0\text{C} /\text{min}$ in oxygen	34

LIST OF SCHEMES

Scheme 2.1: Synthetic Method of Perylene dyes	8
Scheme 2.2: the Synthesis of PDIs with different substituents on both imide and bay position	10
Scheme 3.1: General Synthesis of Ty-B-PDI	18
Scheme 3.2: Synthesis of Ty-B-PDA	19
Scheme 3.3: Synthesis of Ty-B-PDI	20

LIST OF SYMBOLS/ABBREVIATION

Å	Armstrong
A	Acceptor
A	Absorption
Br-PDA	Brominated Perylene dianhydride
C	Concentration
D	Donor
DMF	N,N'-dimethylformamide
DMSO	Dimethyl sulfoxide
DSC	Differential scanning calorimetry
DSSC	Dye sensitized Solar Cell
E _s	Singlet energy
ε	Molar Absorption coefficient
ε _{max}	Maximum Extinction coefficient/Absorptivity
eV	Electron volt
f	Oscillator strength
FT-IR	Fourier Transform Infrared Spectroscopy
Fig.	Figure
hν	Radiation
HOMO	Highest occupied molecular orbital
IR	Infrared spectrum/spectroscopy
K	Kelvin
KBr	Potassium bromide
Kcal	Kilocalorie

LUMO	Lowest unoccupied molecular orbital
M	Molar concentration
MS	Mass spectroscopy
max	Maximum
mol	mole
NMR	Nuclear Magnetic Resonance spectroscopy
nm	nanometer
NPM	N-methylpyrrolidinone
PDA	perylene-3,4,9,10-tetracarboxylic dianhydride
PDI	Perylene diimide
Ty-B-PDA	Tyramine bay substituted perylene-3,4,9,10-tetracarboxylic dianhydride
Ty-B-PDI	Tyramine bay substituted perylene diimide
T_d	Decomposition temperature
TGA	Thermogravimetric Analysis
UV	Ultraviolet
UV-vis	Ultraviolet and visible light Absorption
λ	Wavelength
λ_{\max}	Maximum wavelength
λ_{exc}	Excitation wavelength
Φ_f	Fluorescence quantum yield
τ_0	Radiative lifetime
$\Delta\bar{\nu}_{1/2}$	Half-width selected Absorption
μm	Micrometer

Chapter 1

INTRODUCTION

1.1 Perylene Dyes

Perylene dyes and pigments have emerged as an important class of Rylene dyes with diverse scientific research field, starting from organic electronics [1], to solar cell research [2] and supramolecular chemistry [3]. The great performance pigments called Perylene dyes, was formed from N,N-disubstituted Perylene diimides (PDIs) or Perylene-3,4,9,10-tetracarboxylic dianhydride [4]. Among the Perylene dyes particularly the 3,4,9,10-perylene tetracarboxylic dianhydride (PDA) has been used as a source compound to synthesized dyes and pigments.

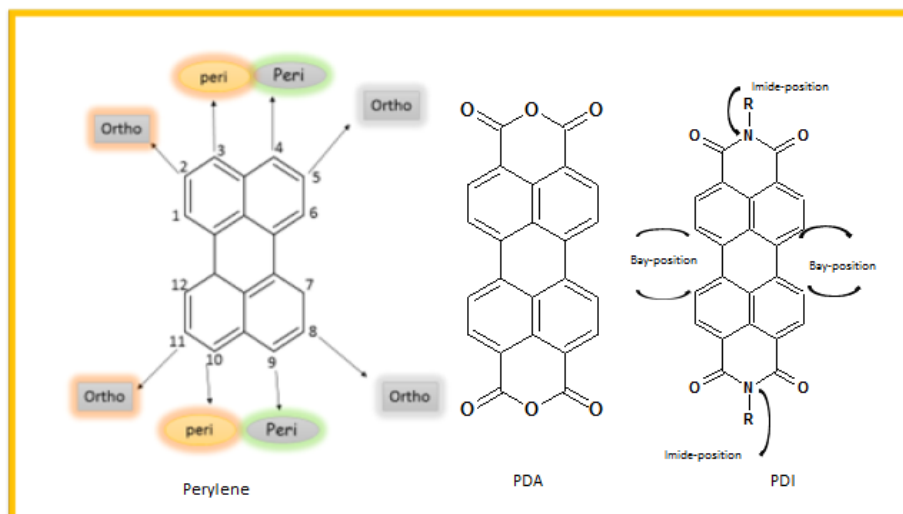


Figure 1.1: A General structure of perylene, PDA and PDI [16]

The modern approach regarding this species of pigments was initially discovered and depicted by M. Kardos from 1912-13 [5]. Additionally, planar π -system of Perylene-

3,4,9,10-tetracarboxylic dianhydride (PDA) in Fig.1.1 above have a rigid structure that has inherently low solubility, due to its strong π - π interaction, and also were used for insoluble organic dyes in automotive paints and engineering resins [6]. Research have shown that most perylene dyes with poor solubility are highly stable photochemically and thermally [7].

However poor solubility in perylene promotes difficulty during purification, synthesis, and Spectroscopy analysis, and also decreases Φ_f by the feasible aggregation from solution. Notably, the basic interest is to get readily synthesized perylene dyes together with great fluorescent quantum yields.

On the other hand, soluble substituents are equally important to optimize the processibility of the rigid structure of PDA. Over the years, PDI were introduced as a dye in textile industries and presently as pigments mostly red, violet and black [8]

(Fig.1.2)

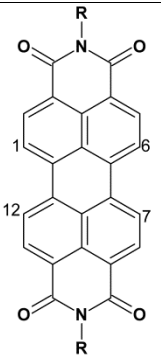
	Substituents on the imide position	Color	Industrial name
	H	Deep red	Pigment violet
	CH ₂ CH ₂ ph	Black	Pigment black 31
	CH ₃	Red	Indanthrene rot 2G

Figure 1.2: Structures of different colored PDI pigments [8]

The basic disparity among the pigments presented in Fig.1.2 rest on substituents of imide position that characterized the significant part for the structural arrangement of the compound together with the device performance.

Usually, the broad Absorption in the visible region couple with high fluorescence quantum yield, excellent photochemical stability along with various fascinating chemical and physical properties of the Perylene diimide played an essential role in an industrial pigment [9]. However, the investigation towards understanding novel-PDI with different chemical and physical properties can be achieved through the synthetic modification on imide position or bay region on core area of PDI in Fig 1.1

1.2 Bay Substituted Perylene Diimide

Expansion of perylene chemistry introduced different useful functionalized position on perylene compounds. These functionalized position of perylene structure are- 2,5,8,11-ortho position, 3,4,9,10- peri-position, and 1,6,7,12-bay position, as presented in Fig. 1.1.

The synthesis of PDIs on a bay region have derived much interest and found wide range applications in many areas of current research due to their outstanding properties [10]. Interestingly, these outstanding electronic and optical properties of PDI has received an excellent applications that consist of organic solar cells [2] Organic Light Emitting Diodes, (OLED) [11], photosensitizers [12], Organic Field Effect Transistors (OFETs) [10], molecular wires [13], logic gates [14] and sensors [15].

Certainly, one of the practical techniques used to generate soluble PDI is the halogenation of bay substituents, this idea results in the distortion on planarity of its

structure that is π - π self-aggregation [16]. Molecular interaction and solubility are two key factors for a solution base supramolecular process. Most successful scientist achieved this by utilizing the side chain substituents that attached on the PDIs. The supramolecular arrangements of semi-conductors are of great important especially in the field of electronic and optoelectronics. However, it is clear that bay functionalization ways is important for controlling the physical and chemical structures of PDI dyes.

Recently, much attention have been focus on 1,7-dibromoperylene tetra carboxylic diimide intermediate, as the best method for the preparation of bay functionalized PDI because of its easy swap of bromo substituent on the bay region with different nucleophiles as presented in Fig. 1.3

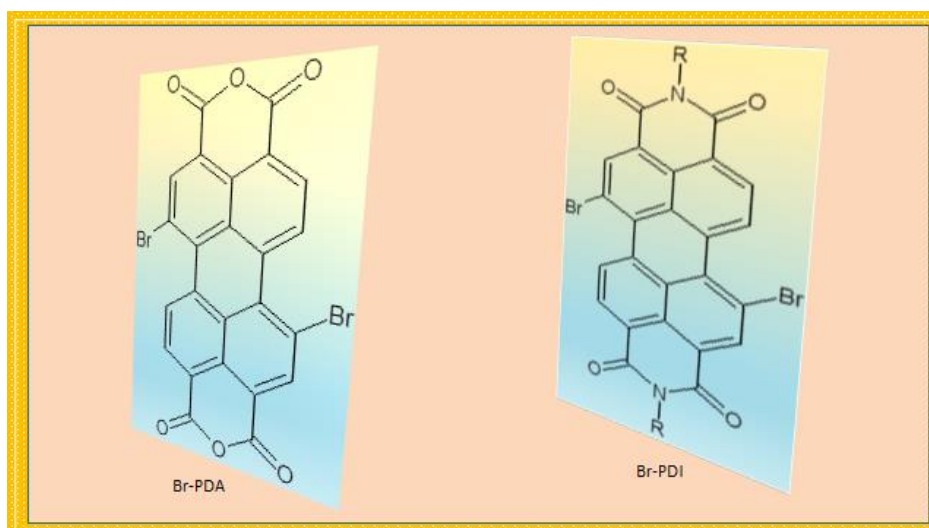


Figure 1.3: The chemical structure of brominated PDA and PDI derivatives. [16]

In general the substituents at bay region of Perylene core has brought about considerable influence on the charge transport properties via modification on

charge reorganization energy, molecular confirmation, also the stacking arrangement [17].

1.3 Electron Transport Properties of Bay Substituted Perylene

Diimide

Oxidation/reduction reactions which transfer electrons from an electron donor molecule to an electron acceptor molecule are said to be an electron transport. The significant requirement in accomplishing an effective and speedy electron transfer is the utilization of the donor-acceptor segments [18]. Scientist have developed a lot of interest in electron donor and acceptor molecules because of their excellent optical and electrical properties including applications in organic photovoltaics, light harvesting, photocatalysis and supramolecular electrons[19]. Recently, research studies have shown that PDIs can also be utilized as a special class of n-type semiconductor in organic electronics [20]. Similarly, joining substituents like chlorine, bromine, fluoride, cyanine etc., to the core area of bay substituted PDIs, has successfully stabilized molecular orbitals and facilitates the electrons transport [21-24].

This novel research, report the synthesis of new class of PDI derivative, Ty-B-PDI, with excellent optical and thermal properties that will emerge as a good candidate for photovoltaic applications. The synthesized product was investigated and characterized by FTIR, UV-vis, emission, TGA, DSC and Elemental Analysis.

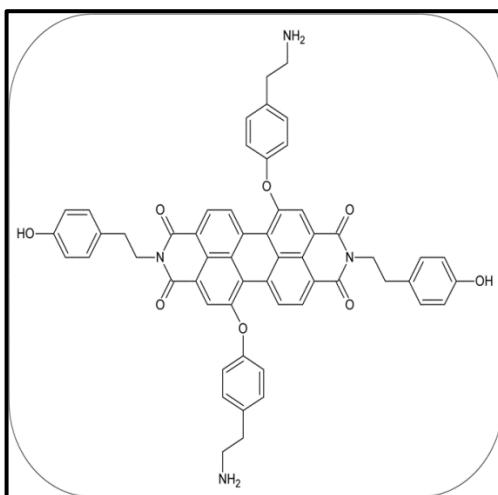


Figure 1.4: Structural representation of bay and imidization position of Ty-B-PDI

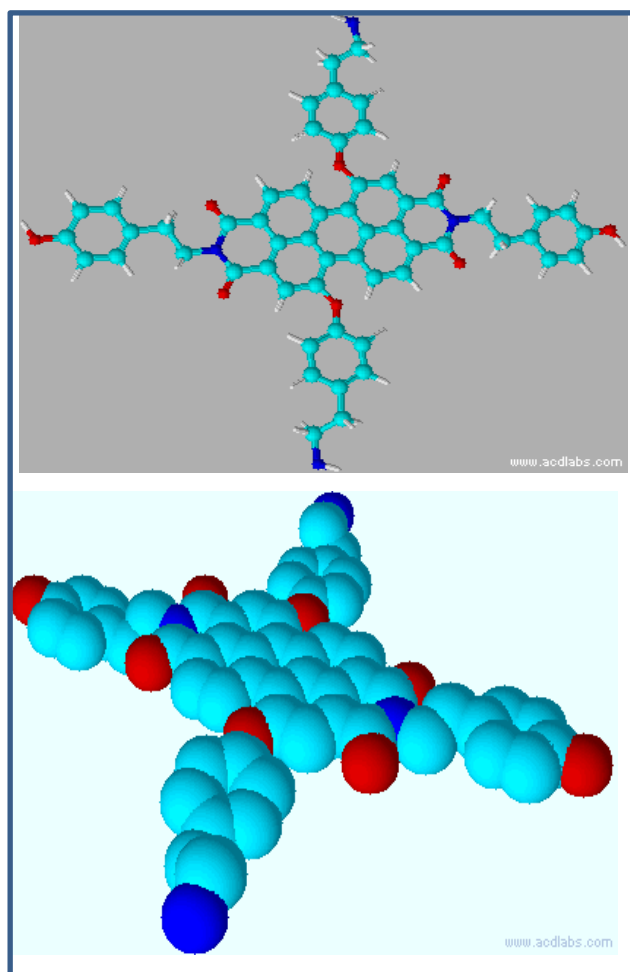


Figure 1.5: 3-D structural representation of bay and imidization position of Ty-B-PDI

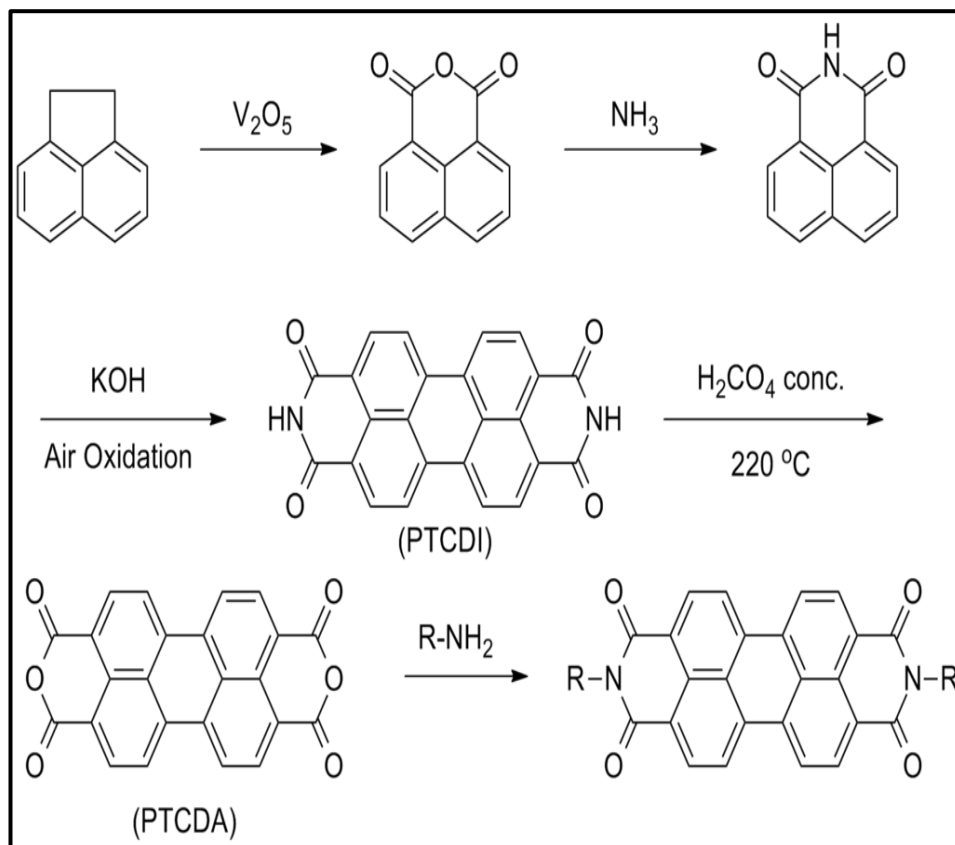
Chapter 2

THEREOTICAL

2.1 Synthesis and Applications of Perylene Dye

The Synthesis of perylene dyes were reported by the pioneer called M. Kardos in 1913. In addition the basic starting raw material of synthesizing PDI derivatives in both laboratory analysis and industrial setting is perylene-3,4,9,10-tetracarboxylic dianhydride (PTCDA). These theoretical positions make an important contribution to our understanding of condensation reaction of PTCDA with aniline or alkyl group, these also account for the development of perylene diimide derivatives in considerable yield [3, 25,] as presented in scheme 2.1.

Evidently, synthetic sequence of PTCDA begins with V_2O_5 -catalyzed air oxidation of acenaphthene which formed naphthalic and afterward treated with NH_3 which proceed to 1,8-naphthalene dicarboxylic imide. The blended 1, 8-naphthalene dicarboxylic imide with potassium hydroxide have formed perylen-3, 4, 9, 10-diimide (PTCDI) at 190-220 $^{\circ}C$, which resulted via air oxidation of smelted reaction compound. PTCDA is further synthesized through hydrolyses of perylene-3, 4, 10-tetracarboxylic diimide with conc. H_2SO_4 at 220 $^{\circ}C$ [7, 26].



Scheme 2.1: Synthetic method of perylene dyes [26]

Interestingly, perylene tetracarboxylic acid diimide, because of its recently enhanced properties, e.g. high photoluminescence quantum yields, strong absorption in visible region, electron accepting features with n-type character, tunable band gap, high thermal, mechanical, chemical and electrochemical stabilities etc., have recorded a great application in the areas of photonic technology, photovoltaic device, organic solar cell, dye lasers, electrophotography, medicine [27-29].

However, the disadvantage of using Perylene dyes involved basically poor solubility owing to strong pi-pi interaction. Solubility of Perylene diimides firmly relies upon substituents together with two approaches that have been proposed to improve the solubility within the organic solvent.

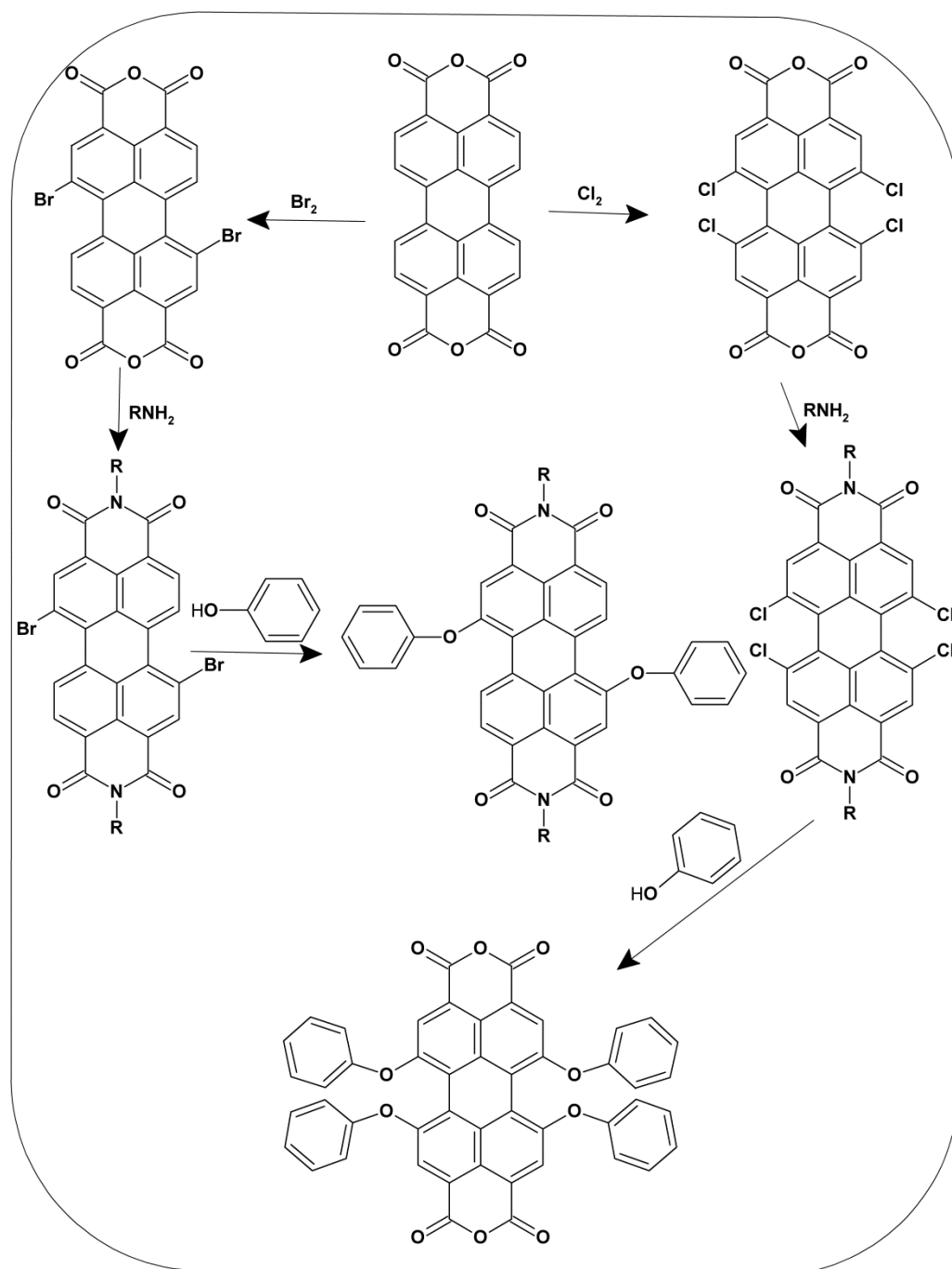
Moreover, the techniques of enhancing the solubility of PDIs consist of two N-substituent on the peri area with two long chain of alkyl groups and Ortho substituted phenyl groups, hence these will be constrained out of the plane of chromophore and by that restrict face to face pi-pi stacking on PDIs. Therefore maintaining the planarity of perylene diimides is fundamental, as peri-position might be the desirable sites for joining the substituents [30].

Another approach for expanding the solubility of the PDIs is the substitution on the bay region (Fig.1.1). Bromination and resulting N-Substitution can prompt 1,6,7,12-tetrabromo-3,4,9,10-Perylene diimides. It is also viable to substitute the bromines with many derivatives e.g. piperidine .due to their bulkiness, the substituents on the bay region influence the aromatic center to curve, which expands the solubility [31].

2.2 Synthesis and Applications of Bay Substituted Perylene Diimides

It can be seen from the above analysis that, the method of synthesizing highly soluble PDIs is by introducing functional group on the bay-position of perylene diimide aromatic centers. The synthesis chemistry of presenting substituents on a bay region which described the functionality of the core area of perylene diimide was discovered in 1980 [32].

As indicated in previous report which shows the phenoxy group in different four positions on the bay position of tetrachloro-substituted perylene diimide through nucleophilic substitution which substitute chlorine molecules in the PDIs (as shown in scheme 2.2).



Scheme 2.2: The synthesis of PDIs with different substituents on both imide and bay position. [33]

Moreover, modern synthesis of bay tetrafluoro substituted PDIs were reasonably synthesized in good yields from the corresponding bay tetrachloro substituted PDIs as starting materials [33]. However, the methodology of four attached chlorination of perylene tetracarboxylic dianhydride was known since 1985 [34]. It was discovered

recently that the most significant procedure of preparing perylene diimides include the utilization of dibromoperylene diimide as intermediate, because of easily swap of bromo-substituent within the core area of PDIs with different nucleophiles [35].

Additionally substitution of halogen atoms in aromatic centers through nucleophilic replacement on bay-position of dibromo-substituted or tetrachloro-substituted PDI is moderately direct; hence the product is isolated in a significant output.

Presently, chloride, bromide, amine, and phenol, base nucleophiles have been attached to PDIs core, prompting to different Perylene derivatives with fascinating electronic and optical components (as presented in scheme 2.2), due to their direct electronic attachments between the novel substituents with the PDI cores. PDIs with good electronic characteristic can as well be adjusted by substituents of conjugated aromatic centers. Taking into account of these principles, PDIs derivatives with electron donating or electron accepting group have been recorded in many literatures. PDIs sometime functions as charge generation materials, singly or alongside other photoconductive dyes and in electrophotography. Another area of application of Perylene derivatives is the use of heterojunctions with phtalocyanines in photoelectrochemical and organic photovoltaic cells. However many records propose that the perylene derivatives usually function as n-type semiconductor [36].

2.3 Electron Transfer

Perylene diimide and naphthalene molecules as donor-acceptor chromophores explained electron transport through intera-intermolecular charge transfer interactions and electron transfer reaction [37].

These parts study some of the principle and theoretical ideas for energy and electrons transfer. The photoinduced energy and electron transfer processes that can bring about between electron rich Donor D and electron deficient Acceptor A in a molecular D to A couple were schematically illustrated in (Fig. 2.1). Electron transfer of donor–acceptor produced $D^+ + A^-$, which originated from Photoexcitation of Donor D^* or Acceptor A^* . Relatively, energy transfer is only possible when the element with the highest optical energy gap, (E_g) is excited.

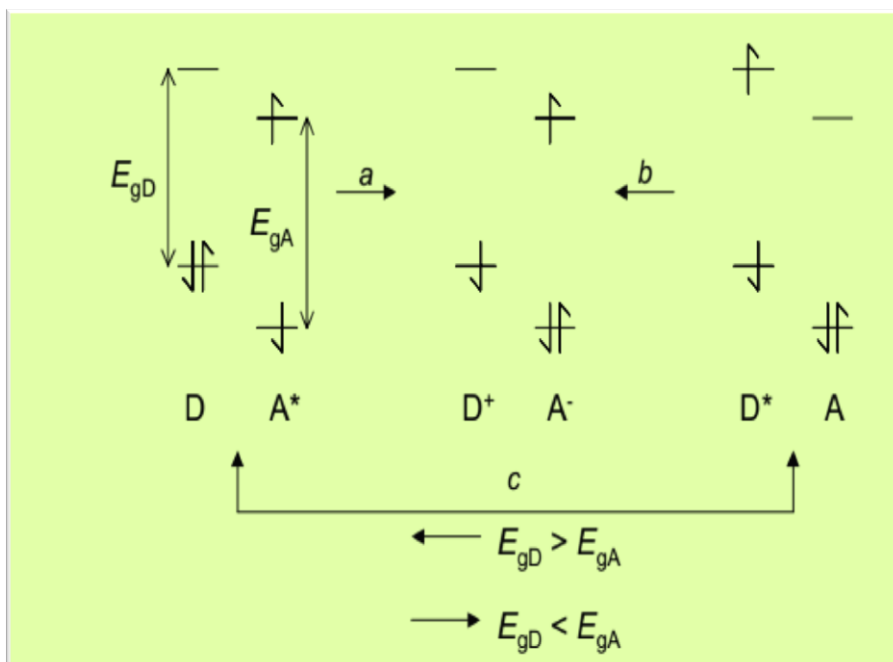


Figure 2.1: Electron transfer between Donor and Acceptor [38]

Normally the redox reaction at a ground state of electrons transfer occurs between donor-acceptor molecules. The differences in the oxidation/reduction potential of donor-acceptor affect the ground state of free-energy changes in the electron transfer process. Due to the extensive HOMO-LUMO breach of organic molecules in the ground state, electrons transfer would be a vast endothermic process.

One of the important properties of organic substance is the electron transport ability, which described the photovoltaic mechanism for producing great charge segregation and effective photovoltaic properties. In general, the intermolecular charge transfer process of the organic molecules have been improved by the electron transfer from donor-acceptor site, and also increases photoinduced electrons that is accountable for revealing great solar to power conversion efficacy in DSSCs [38].

2.4 Organic Solar Cells and Their Applications

The current age of organic photovoltaic consist of an extensive variety of promising solar modernization that contain nanocrystalline photo electrochemical cells, DSSCs, polymer solar cells.

Similarly, Organic photovoltaics offer novel fields of energy production. Smooth roll-to-roll processing that can produce vast scale together with inexpensive modules. Hence approved energy conversion effectiveness equal to 8.3% have been attained on less substrates [39]. Organic photovoltaics utilize semiconducting polymers as light harvesting materials.

Previously, much research work has focus on the advancement, of organic photovoltaics because of its rapid improved efficiency, cost efficiency, energy harvesting, smooth processing agreeable by flexible substrates. Numerous powerful techniques have been also investigated to enhanced the performance of photovoltaics via the synthesis of novel limited energy gap (band gap) material for excellent photo assembling, design of new arrangements cell, interfacial adjustments for excellent charge transport collection, and improvement of stage separation in bulk hetrojunction (BHJ) layers [40.]

Generally, the usual setup of Organic Solar Cells (OSCs) are invented in an effective Bulk Heterojunction (BHJ) layers and planner heterojunction layers introduced by high work function and crystalline metal oxide for the base anode and low work capacity metal for the high cathode. In order to obtain effective charge aggregation, work function of cathode and anode ought to be coordinated to the donor of high occupied molecular orbitals HOMO with acceptor of lowest unoccupied molecular orbital (LUMO) respectively. Low work function metals as the top cathode have been chosen for better coordinating with the LUMO of acceptor. Nevertheless, metals with low work function are not greatly steady as the top cathode because of the sensitiveness to moisture in air and oxygen [41-42]. So to secure top cathode, bi-layered metals for example Mg/Al or Ca/Al have been utilized as blended cathode for the performance upgrade organic light emitting diodes and in Organic Solar cells [43-44].

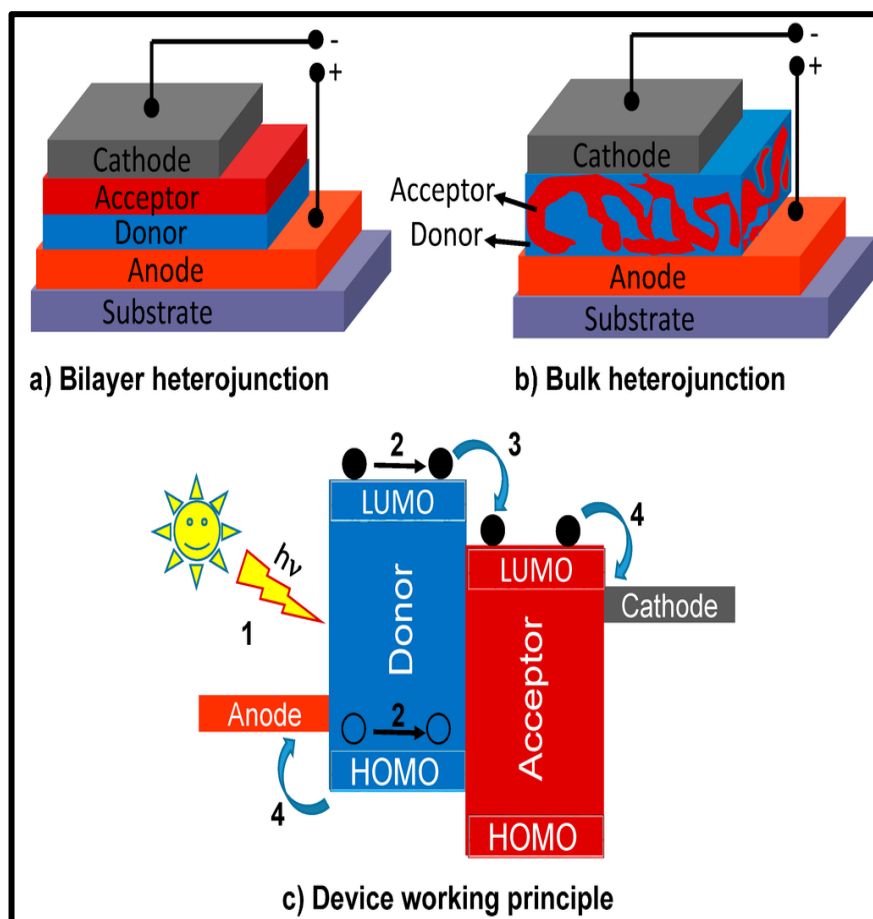


Figure 2.2: The devices system of a) Bilayer heterojunction, b) Bulk heterojunction, c) Working principle of the device. [43-44].

In essence the perfect generation process for organic solar cells (OSCs) will be solution procedure, where the diverse cell layers are placed on to pliable substrates to tailor for a highest easy roll-to-roll class of printing. Also the organic solar cells ought to keep up high tools stability and effectiveness over a specific time frame. Basically the inverted arrangement of organic solar cells might be the most excellent candidate to confront all these requirements which comprise stability, high efficiency, low cost and rapid production into one framework.

Recently, perylene diimides polymers were also found to be a new acceptor substance that can replaced fullerene derivatives which have a wide range train that promote the usefulness of an organic solar cells, such as absorption of light via

photoactive layer, charge transfer and movement of exciton from the interface, charge segregation at coulomb fascination and isolated charges are carried to a cathode. Chemically modified fullerene derivatives that absorb just a small part of sunlight of spectral scope over 500nm with acceptors is an objective way to increase the absorption of photoactive layer. Perylene dyes is an outstanding class of new acceptor materials because of their recently promising energy conversion effectiveness up to 4% in blend with low energy gap polymers [45] and molecules.

However powerful Absorption in the visible region of PDI offers advantages, for example optimum electron transport properties, flexible synthetic potential outcomes to adjust energy levels, solubility, stacking conduct, excellent thermal and photostability [46].

Chapter 3

EXPERIMENTAL

3.1 Materials

1,7-dibromoperylene-3,4,9,10-tetracarboxylic dianhydride, 4-(2-aminoethyl)phenol, potassium carbonate (K_2CO_3), dimethylformamide(DMF), isoquinoline, acetic acid, methanol, ethanol, diethylether, trichloroethylene, dimethylsulphureoxide (DMSO), dichloromethane, N-methylperodine, and m-cresol, were utilized directly as received, whereas acetone and chloroform were distilled before used. The chemicals were obtained from the company called Sigma Aldrich.

3.2 Instruments

The measurements of IR spectra were recorded using JASCO FT-IR-6200 with KBr pellets. Also the measurements of UV-visible spectra were obtained via Cary-100 spectrophotometer, fluorescence quantum yield and emission spectra were measured by Varian Eclipse Fluorescence spectrophotometer DSC Model, Jade DSC instruments were used for DSC analysis at the heating $10^0C/min$ in nitrogen, Thermogravimetric thermograms were recorded using a perkin Elmer,pyris 1 TGA, at heating rate of $10^0C /min$ in oxygen and elemental analysis were recorded from a Carlo-Erba-1106 C H N analyzer.

3.3 Method of Synthesis

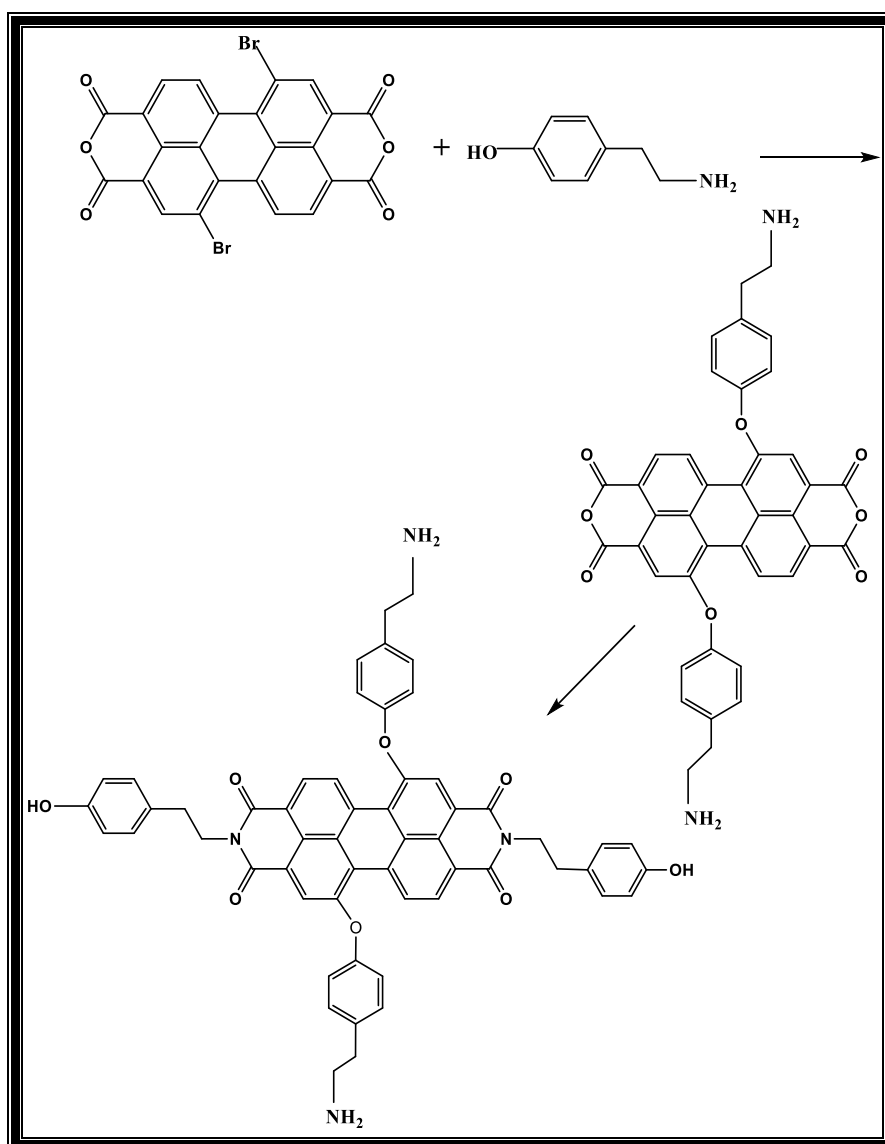
This part describes the synthesis of bay substitution and imidization of brominated perylene dianhydride. The synthesis was successfully carried out through condensation of 4-(2-aminoethyl) phenol with 1,7-dibromoperylene-3,4,9,10-

tetracarboxylic dianhydride (Br-PDA) using DMF and isoquinoline as a solvent.

Below is the overall synthesis of the compound.

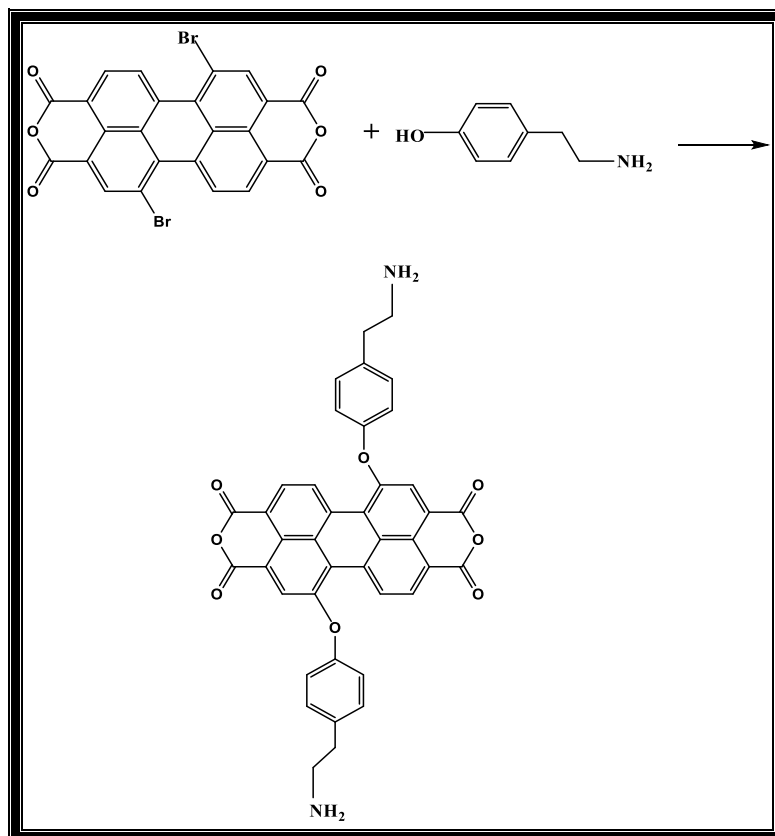
3.4 General Synthesis of Ty-B-PDI

A novel class of perylene derivative Ty-B-PDI was synthesized via two steps as in scheme 3.1.



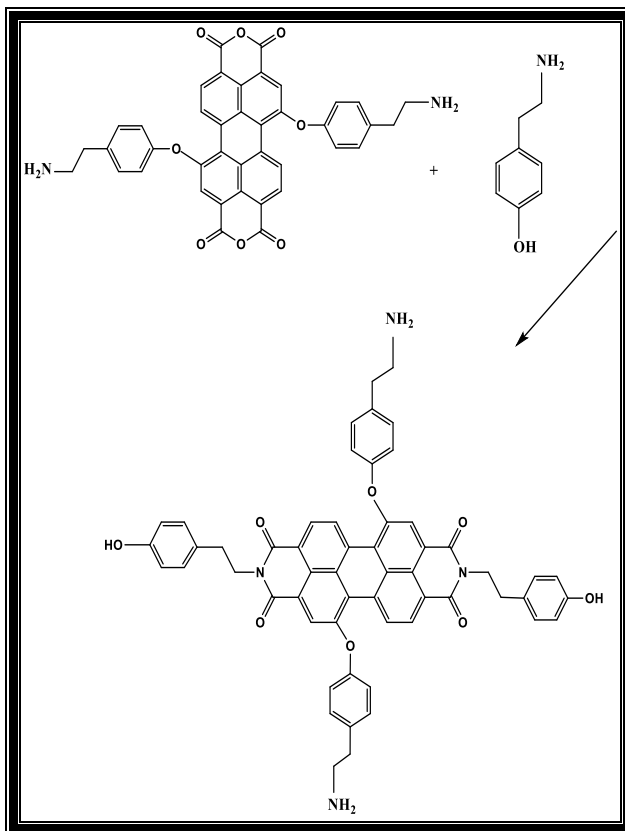
Scheme 3.1: General synthesis of Ty-B-PDI

The compound was first synthesized by the reaction between the chromophore, 1,7-dibrominated perylene-3,4,9,10-tetracarboxylic dianhydride (Br-PDA) and tyramine (scheme 3.2).



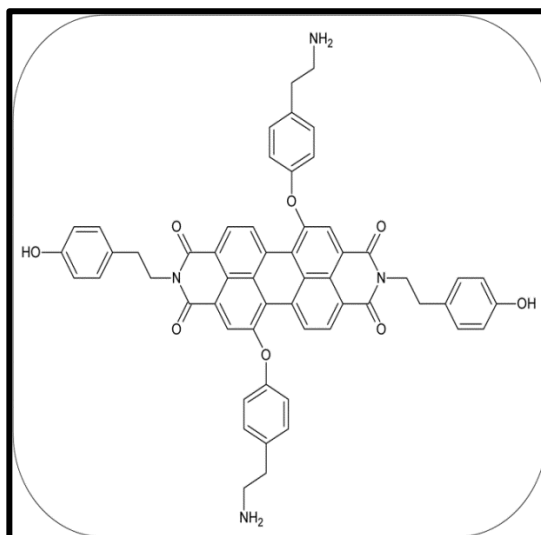
Scheme 3.2: Synthesis of Ty-B-PDA

A novel class of perylene derivative was finally synthesized with addition of tyramine to the imide position (scheme 3.3)



Scheme 3.3: Synthesis of Ty-B-PDI

3.5 Synthesis of Ty-B-PDI



A solution of 1,7-dibromoperylene-3,4,9,10-tetracarboxylic dianhydride (1.0g ,1.8mmol), 4-(2-aminoethyl)phenol (0.749g, 5.46mmol), and Potassium carbonate (K_2CO_3) (0.6219 g, 4.5 mmol) in 67 ml of DMF were brought to reflux at 150^oC under argon atmosphere with stirring for 14 hrs and (0.746 g, 5.46 mmol) 4-(2-aminoethyl)phenol was added again and refluxed to 150 ^oC under argon atmosphere with stirring for another 10 hrs. The reaction mixture was then poured and cooled into a solution of 60 ml of acetic acid and 60 ml of water and put in to refrigerator for one week. The mixture was filtered by vacuum filtration and treated first with water for good 34 hrs. to remove the acetic acid and followed by ethanol for 51 hrs in a soxhlet set up in order to remove the unreacted amine. The reaction was control by thin layer chromatography (TLC). Also 1.0 g of the product was weight and dissolved in 25 ml of isoquinoline with 1ml of amide in a reaction mixture under argon atmosphere with stirring at 120 ^oC for 4 hrs. 150 ^oC for 3 hrs., 180 ^oC for 2 hrs. and 200 ^oC for 1 hr. The product was poured in to required volume of diethylether and put into refrigerator for 24 hrs. in order to form precipitate. The precipitate was purified with Chloroform soxhlet for complete 60 hrs. The purified product was dried under vacuum at 100 ^oC.

Yield 80%; **Color:** dark red.

IR (KBr, cm^{-1}); $\nu = 3422, 3017.)$; 2919, 2844, 1696, 1653, 1584, 1510, 1344, 1157, 805.

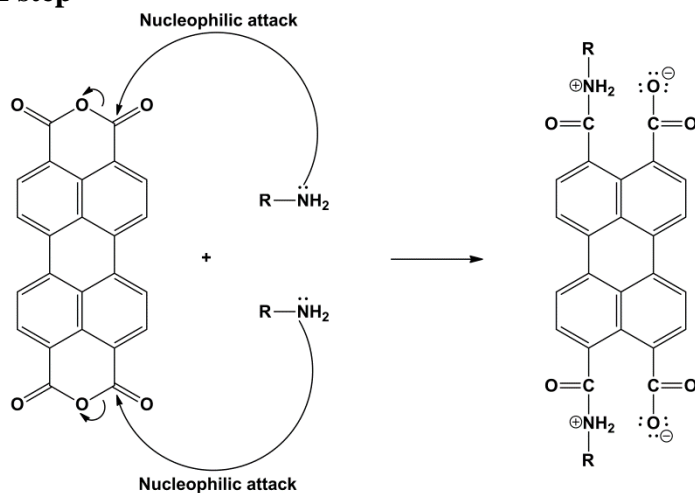
UV-vis (DMF): λ_{max} (nm) = 460, 490, 525. Fluorescence (DMF): λ_{max} (nm) = 545, 578, and $\Phi_f = 0.1$.

Anal. calcd for for $C_{56}H_{44}N_4O_8$ (M_w , 900.97): C, 74.65; H, 4.92; N, 6.22. **Found:** C, 73.71; H, 4.68; N, 6.14.

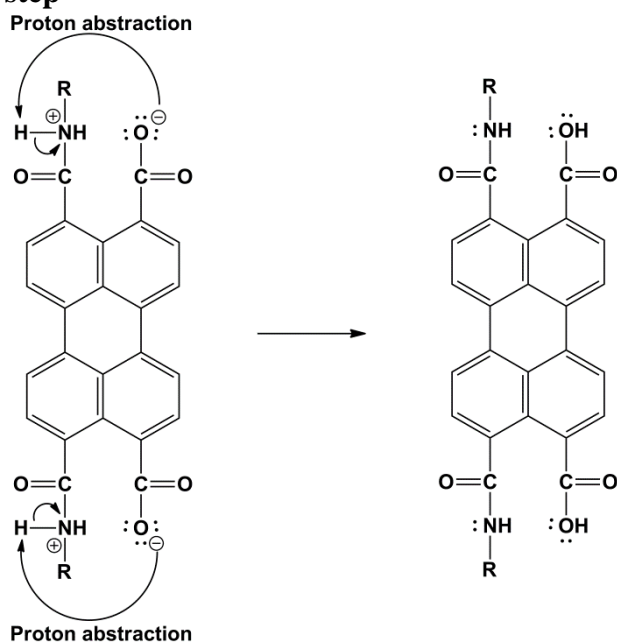
3.6 General Reaction Mechanism of Perylene Diimide

Below is the general steps involved in synthesis mechanism of Perylene diimide which mainly focus on nucleophilic attack and proton abstraction.

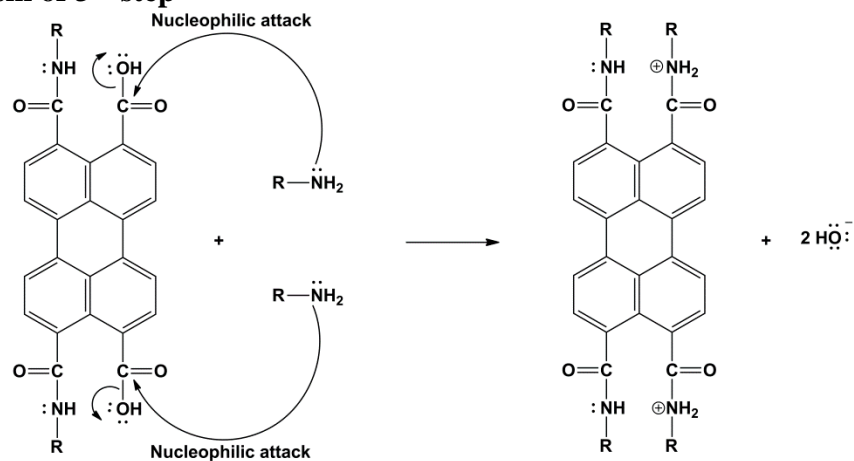
Mechanism 1st of step



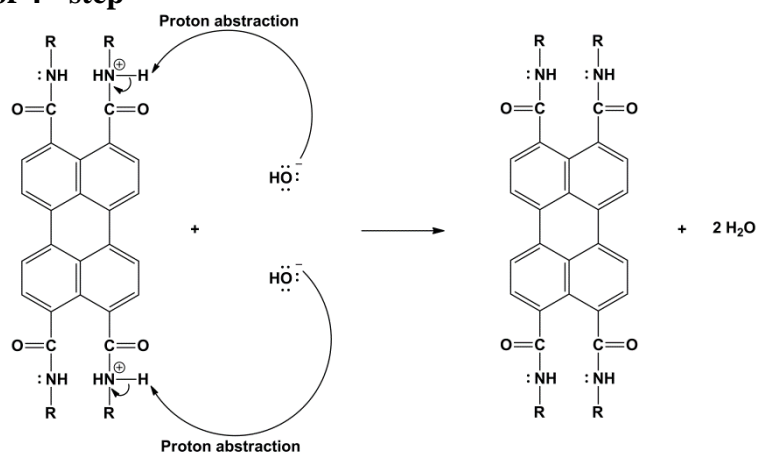
Mechanism of 2nd step



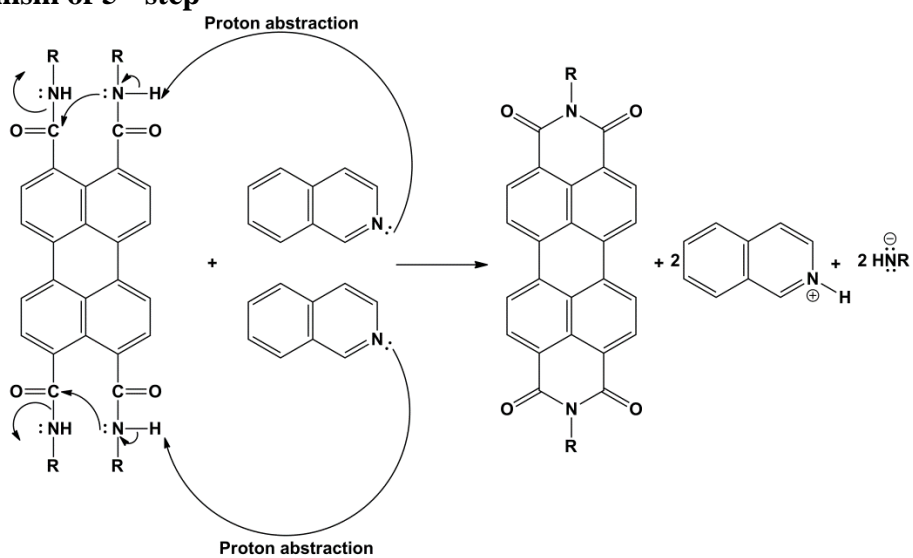
Mechanism of 3rd step



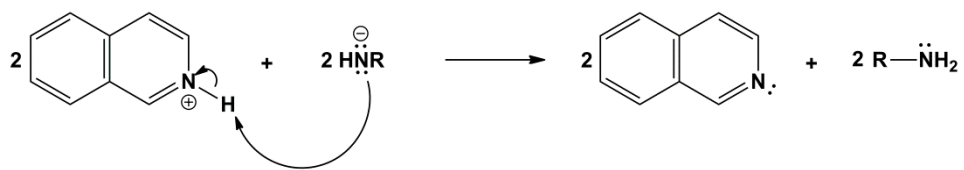
Mechanism of 4th step



Mechanism of 5th step



Mechanism of 6th step



Chapter 4

DATA AND CALCULATION

4.1 Optical and Photochemical Properties

4.1.1 Molar Absorption Coefficient (ϵ_{max})

Molar absorption coefficient is one of the parameter that defined how strongly a substance absorbed light at a given wavelength. It is an intrinsic property of a species. Generally, absorbance (A) of a sample is depend on the concentration (C) and pathlength(l) of the species through the beer-lambert law as shown below

$$\epsilon_{max} = \frac{A}{Cl}$$

Where

ϵ_{max} Molar extinctions coefficient of a selected absorption wavelength

l path length

A Absorbance

C Concentration

absorption spectrum of Ty-B-PDI in (Fig.4.5-4.9) shows the absorption value of 0.70, 0.90, 0.25 at maximum wavelength (λ_{\max} = 525, 527, 535nm) for the concentration of $1.0 \times 10^{-5} \text{ mol L}^{-1}$ and path length of 1cm.

However, the ϵ_{\max} of Ty-B-PDI in DMF is calculated below

$$\epsilon_{\max} = \frac{0.70}{1 \times 1.0 \times 10^{-5}} = 70000 \text{ mol}^{-1} \text{ cm}^{-1}$$

ϵ_{\max} of Ty-B-PDI in DMF is $70000 \text{ mol}^{-1} \text{ cm}^{-1}$

Similarly, the values of ϵ_{\max} of Ty-B-PDI in various solvents were calculated and presented in table 4.1

Table 4.1.1: Molar absorption coefficients of Ty-B-PDI in various solvents

Solvents	λ_{\max} (nm)	A	ϵ_{\max} ($\text{L mol}^{-1} \text{ cm}^{-1}$)
DMF	525	0.70	70000
NMP	527	0.90	90000
TFA	535	0.25	25000

4.1.2 Fluorescence Quantum Yield (Φ_f)

When light strike a fluorophore or chromophore therefore photon of light absorbed by exciting of an electrons from its lowest energy level to high energy level. This species have different fate depending on the exact nature of the fluorophore or chromophore and its surrounding. Beside the outcome is deactivated (loss of energy) and return to ground state. In general, fluorescence quantum yield Φ_f is the ratio of photon absorbed and emitted via fluorescence. On the other hand the quantum yield Φ_f provides the possibility of the excited state to be deactivated by fluorescence instead of non-radiative mechanism.

The comparative methodology for recording of Φ_f involved the application of well characterized standard samples with known Φ_f values.

Basically, the identical absorbance at equal excitation wavelength with solutions of the standard and test samples can be presumed to be absorbing equal number of photons. Hence, easy proportion of cohesive fluorescence intensities of solutions that reported under the same conditions can produce the ratio of the quantum yield values. However it is irrelevant to compute the Φ_f for the test sample since Φ_f for the standard sample is known. The unknown quantum yield in respect to the standard is the proportion of the integrated band regions under the two fluorescence spectra after they have been optimized for the detector reaction function. The known quantum yield standard is multiplied and gives the absolute quantum yield of the unknown

$$\Phi_f = \frac{A_s}{A_u} \times \frac{S_u}{S_s} \times \left[\frac{n_u}{n_s} \right]^2 \times \Phi_s$$

Where

A_s Standard absorbance of reference compound

Φ_f Unknown quantum yield

n_u Unknown refractive index of a solvent

S_u integral emission area of unknown band

Φ_s standard quantum yield of reference solvent

A_u Absorbance of unknown sample

n_s Standard refractive index of solvent

S_s Integral emission area across the standard band

N,N-didodecyle-3,4,9,10-perylenebis (dicarboxyimide) published by ICIL in 1996 with $\Phi_f = 1$ in trichloromethane was taken as a reference for the measurements of Φ_f in perylene derivatives [47]. Emission spectra of the excitation wavelength of a compound at $\lambda_{exc} = 485\text{nm}$ was applied. The Absorption of a reference solution and the sample was adjusted to 0.1 at excitation of wavelength in order to reduce any effect from re-absorption. The table below gives Φ_f values of a compound by using the above relationship.

Φ_f Calculation of Ty-B-PDI in DMF

$\Phi_s = 1$ in chloroform

$$n_u = 1.4305$$

$$n_s = 1.4458$$

$$A_s = 0.1003$$

$$A_u = 0.1005$$

$$S_u = 66.566$$

$$S_s = 851.81$$

$$\Phi_f = \frac{0.1003}{0.1005} \times \frac{66.566}{851.81} \times \left[\frac{1.4305}{1.4458} \right]^2 \times 1 = 0.076 \cong 0.1$$

Table 4.1.2: Fluorescence quantum yield of Ty-B-PDI

Solvent	n_u	A_u	S_u	A_s	S_s	Φ_f
DMF	1.4305	0.1005	66.566	0.1003	851.81	0.10
NMP	1.470	0.1018	65.024	0.1003	851.81	0.08

4.1.3 Half-width of the Selected Absorption ($\Delta\bar{\nu}_{1/2}$)

The selected half-width absorption is defined as full or half-width of the curve at the half of the maximum intensity. Generally, the half-width of the selected maximum absorption can be determine using the relationship below

$$\Delta\bar{\nu}_{1/2} = \bar{\nu}_i - \bar{\nu}_{ii}$$

Where,

$\bar{\nu}_i - \bar{\nu}_{ii}$ Frequencies of Absorption spectrum

$\Delta\bar{\nu}_{1/2}$ selected maximum absorption of half-width

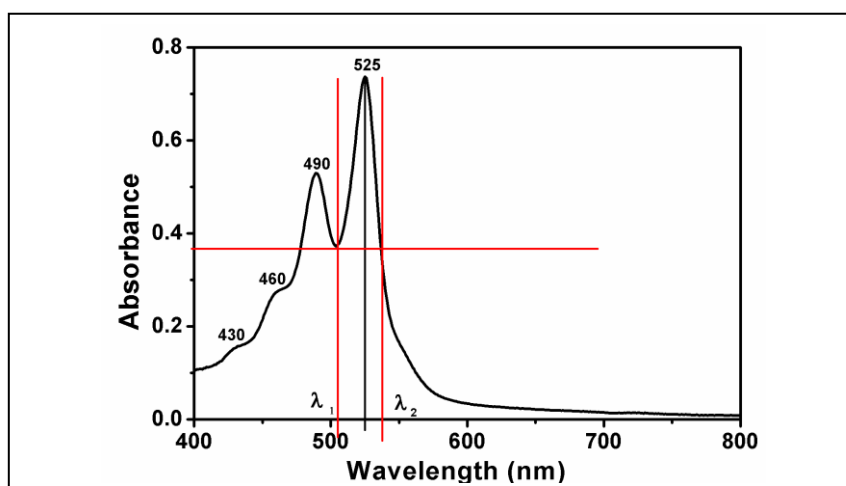


Figure 4.1: Half-Width plots on the absorption spectrum of Ty-B-PDI in DMF

The value of $\Delta\bar{\nu}_{1/2}$ From Fig. 4.1 were calculated and presented in table 4.3

By using this formula $\Delta\bar{\nu}_{1/2} = \bar{\nu}_i - \bar{\nu}_{ii}$ and $\bar{\nu}_i = \frac{1}{\lambda}$

$$\text{at } \lambda_i = 520 \text{ nm} \times \frac{10^{-9} \text{ m}}{1 \text{ nm}} \times \frac{100 \text{ cm}}{1 \text{ m}} = 5.2 \times 10^{-5} \text{ cm}$$

$$\bar{\nu}_i = \frac{1}{5.2 \times 10^{-5} \text{ cm}} = 19230.77 \text{ cm}^{-1}$$

$$\text{at } \lambda_{ii} = 538 \text{ nm} \times 10^{-9} \frac{\text{ m}}{1 \text{ nm}} \times \frac{100 \text{ cm}}{1 \text{ m}} = 5.38 \text{ cm}$$

$$\bar{\nu}_{ii} = \frac{1}{5.38 \times 10^{-5}} = 18587.36 \text{ cm}^{-1}$$

$$\Delta\bar{\nu}_{1/2} = 19230.77 \text{ cm}^{-1} - 18587.36 \text{ cm}^{-1} = 643.41 \text{ cm}^{-1}$$

Table 4.1.3: Half-width of the selected maximum absorption of Ty-B-PDI

Solvents	λ_i (nm)	λ_{ii} (nm)	$\Delta\bar{\nu}_{1/2}$ (cm^{-1})
DMF	520	538	643.41
NMP	521	535	502.27
TFA	528	541	455.10

4.1.4 Theoretical Radiative Lifetime (τ_0)

The theoretical radiative lifetime is refers to theoretical lifetime of an excited molecule for extinction of radiationless transitions. The equation below is used to calculate the theoretical radiative lifetime [48].

$$\tau_0 = \frac{3.5 \times 10^8}{\bar{\nu}_{\max}^2 \times \epsilon_{\max} \times \Delta\bar{\nu}^{1/2}}$$

Where

$\Delta\bar{\nu}_{1/2}$ selected Absorption half-width

ϵ_{\max} molar extinction co-efficient at selected absorption wavelength

$\bar{\nu}_{\max}$ mean frequency for the absorption band

τ_0 Radiative lifetime

The formula above is used to estimate radiative lifetime of the synthesized Ty-B-PDI compound in various solvents as presented in table 4.4

Theoretical lifetime of Ty-B-PDI in DMF

From fig.4.1 and 4.5 $\lambda_{\max} = 525\text{nm}$, $\Delta\bar{\nu}_{1/2} = 643.41\text{cm}^{-1}$, $\epsilon_{\max} = 70000 \text{ mol}^{-1}\text{cm}^{-1}$

$$\text{at } \lambda_{\max} = 525\text{nm} \times \frac{10^{-9}\text{m}}{1\text{nm}} \times \frac{100\text{cm}}{1\text{m}} = 5.25 \times 10^{-5}\text{cm}$$

$$\bar{\nu} = \frac{1}{5.25 \times 10^{-5}} = 19047.62 \text{ cm}^{-1}$$

$$\tau_0 = \frac{3.5 \times 10^8}{(19047.62\text{cm}^{-1})^2 \times 70000\text{mol}^{-1}\text{cm}^{-1} \times 643.41 \text{ cm}^{-1}} = 2.142 \times 10^{-8}\text{s}$$

$$\tau_0 = 21.42 \times 10^{-9}\text{s} \times \frac{1\text{ns}}{10^{-9}\text{s}} = 21.42\text{ns}$$

Table 4.1.4: Theoretical radiative lifetime of Ty-B-PDI in different solvents

Solvent	λ_{\max} (nm)	ϵ_{\max} (L mol ⁻¹ cm ⁻¹)	$\bar{\nu}_{2\max}$ (cm ⁻²)	$\Delta\bar{\nu}_{1/2}$ (cm ⁻¹)	τ_0 (ns)
DMF	525	70000	3.62×10^8	643.41	21.42
NMP	527	90000	3.60×10^8	502.27	21.50
TFA	535	25000	3.49×10^8	455.10	88.05

4.1.5 Theoretical Fluorescence Lifetime (τ_f)

The theoretical fluorescence lifetime is a measure of the time stays in the excited state before fluorescence by emitting a photon [49]. The lifetimes of chromophore ranged from picoseconce to nanoseconds, and it can be determine by the given equation below

$$\tau_f = \tau_0 \times \Phi_f$$

Where

Φ_f = Fluorescence quantum yield

τ_f = Fluorescence lifetime

τ_0 = Radiative lifetime

The calculated values of theoretical fluorescence lifetime in various solvents were illustrated below.

Table 4.1.5: Theoretical fluorescence lifetime of Ty-B-PDI

Solvents	Φ_f	τ_0 (ns)	τ_f (ns)
DMF	0.10	21.42	1.63
NMP	0.08	21.50	1.72

4.1.6 Fluorescence Rate Constants K_f

The equation below is used to determine the Fluorescence rate constants.

$$k_f = \frac{1}{\tau_0}$$

Where

τ_0 = Radiative lifetime (s)

K_f = Fluorescence rate constants (s^{-1})

Fluorescence rate constants K_f in DMF

$$\tau_0 = 21.42\text{ns} = 21.42 \times 10^{-9}\text{s}^{-1} \text{ or } 2.142 \times 10^{-8}\text{s}^{-1}$$

$$K_f = \frac{1}{2.142 \times 10^{-8}} = 4.66 \times 10^7\text{s}^{-1}$$

The table 4.6 below gives the calculated values of fluorescence rate Constants

Table 4.1.6: Fluorescence Rate Constants data of Ty-B-PDI.

Solvents	τ_0 (ns)	K_f (s^{-1})
DMF	21.42	4.66×10^7
NMP	21.15	4.65×10^7
TFA	88.05	1.14×10^7

4.1.7 Rate Constants of Radiationless Deactivation (k_d)

The equation below is used to determine the rate constants of radiationless deactivation value

$$k_d = \left(\frac{k_f}{\Phi_f} \right) - k_f$$

Where

K_f Fluorescence rate constant (s^{-1})

K_d rate constant of radiationless deactivation (s^{-1})

Φ_f Fluorescence quantum yield

Table 4.1.7: Rate constants of radiationless deactivation

Solvent	Φ_f	K_f (s^{-1})	K_d (s^{-1})
DMF	0.10	4.66×10^7	5.359×10^8
NMP	0.08	4.65×10^7	6.132×10^8

4.1.8 Oscillator Strengths (f)

Oscillator Strength in spectroscopy is a dimensionless quantity that shows the possibility of Absorption or emission within electromagnetic radiation in transitions of energy level. Oscillator strengths can be calculated using the equation below [48]

$$f = 4.32 \times 10^{-9} \Delta\bar{\nu}_{1/2} \epsilon_{\max}$$

where

$\Delta\bar{\nu}_{1/2}$ Half-width of the selected absorption

f Oscillator strength

ϵ_{\max} molar extinction coefficient at the selected absorption wavelength

The Oscillation strength of Ty-B-PDI in DMF

$$\Delta\bar{\nu}_{1/2} = 643.41 \text{ cm}^{-1}$$

$$\epsilon_{\max} = 70000 \text{ Lmol}^{-1}\text{cm}^{-1}$$

$$f = 4.32 \times 10^{-9} \times 643.41 \times 70000 = 0.19$$

The calculated values of Oscillation strength in various solvents of Ty-B-PDI, were shown in table 4.8

Table 4.1.8: Oscillator strengths data of Ty-B-PDI

Solvent	$\Delta\bar{\nu}_{1/2} \text{ cm}^{-1}$	$\epsilon_{\max} \text{ Lmol}^{-1}\text{cm}^{-1}$	f
DMF	643.41	70000	0.194
NMP	502.27	90000	0.195
TFA	455.10	25000	0.049

4.1.9 Singlet Energies (Es)

Theoretically, the relationship shown below is used to determine the energy needed to promote electrons from ground state to excited state.

$$E_S = \frac{2.86 \times 10^{-5}}{\lambda_{\max}}$$

Where

λ_{\max} maximum Absorption wavelength (Å)

E_S Singlet energy (kcal mol⁻¹)

Singlet energy of Ty-B-PDI was calculated using above relationship and the data was given in the table 4.9 below.

Singlet energy in DMF

$$\text{at } \lambda_{\max} = 525 \text{ nm} \times \frac{10^{-9} \text{ m}}{1 \text{ nm}} \times \frac{1 \text{ \AA}}{10^{-10} \text{ m}} = 5250 \text{ \AA}$$

$$E_S = \frac{2.86 \times 10^{-5}}{5250} = 54.47 \text{ kcal/mol}$$

Table 4.1.9: Singlet energies data of Ty-B-PDI

Solvent	λ_{\max} (Å)	E_S (kcal mol ⁻¹)
DMF	5250	54.47
NMP	5270	54.25
TFA	5350	53.45

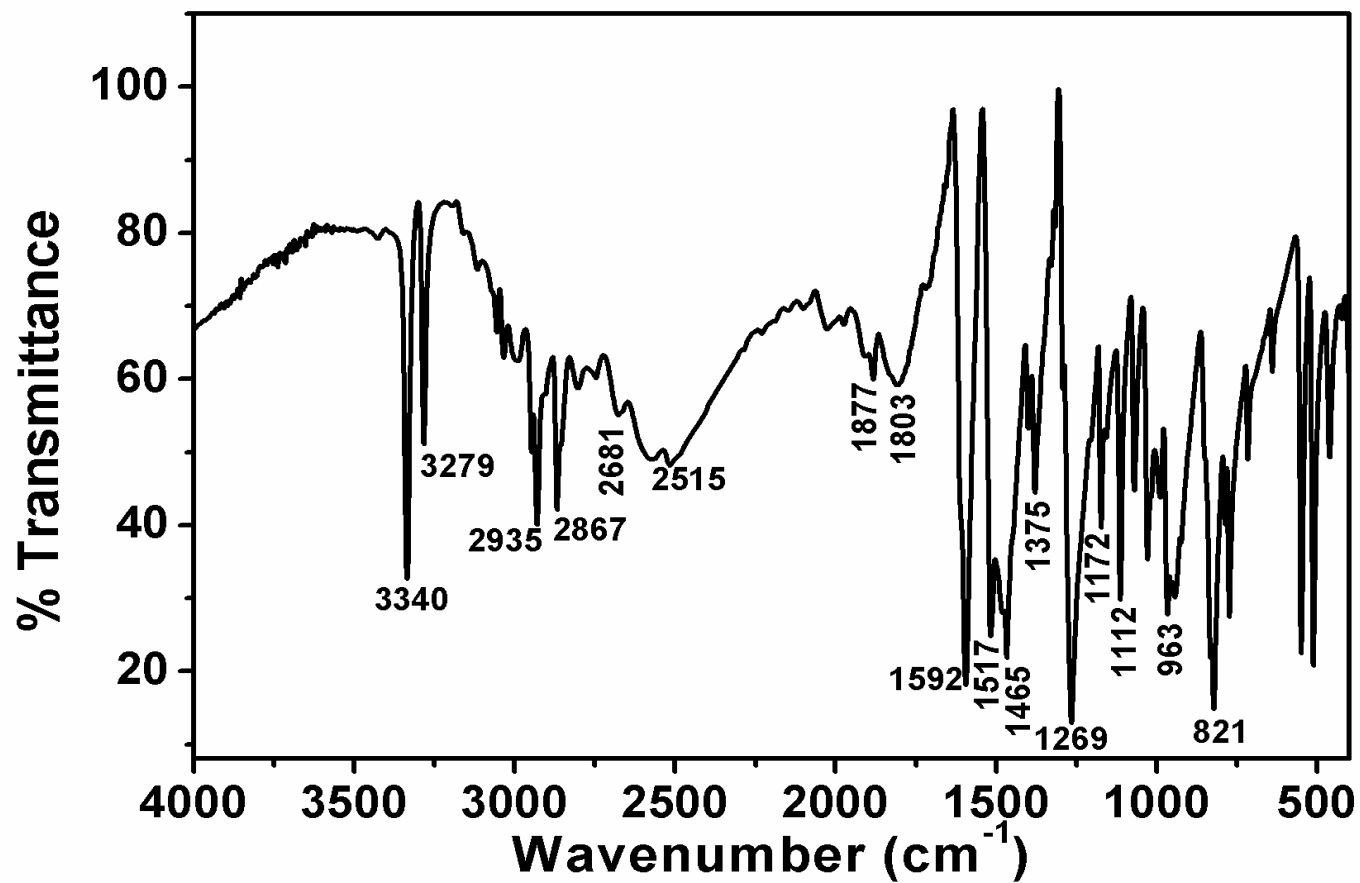


Figure 4.2: FTIR spectrum of Tyramine

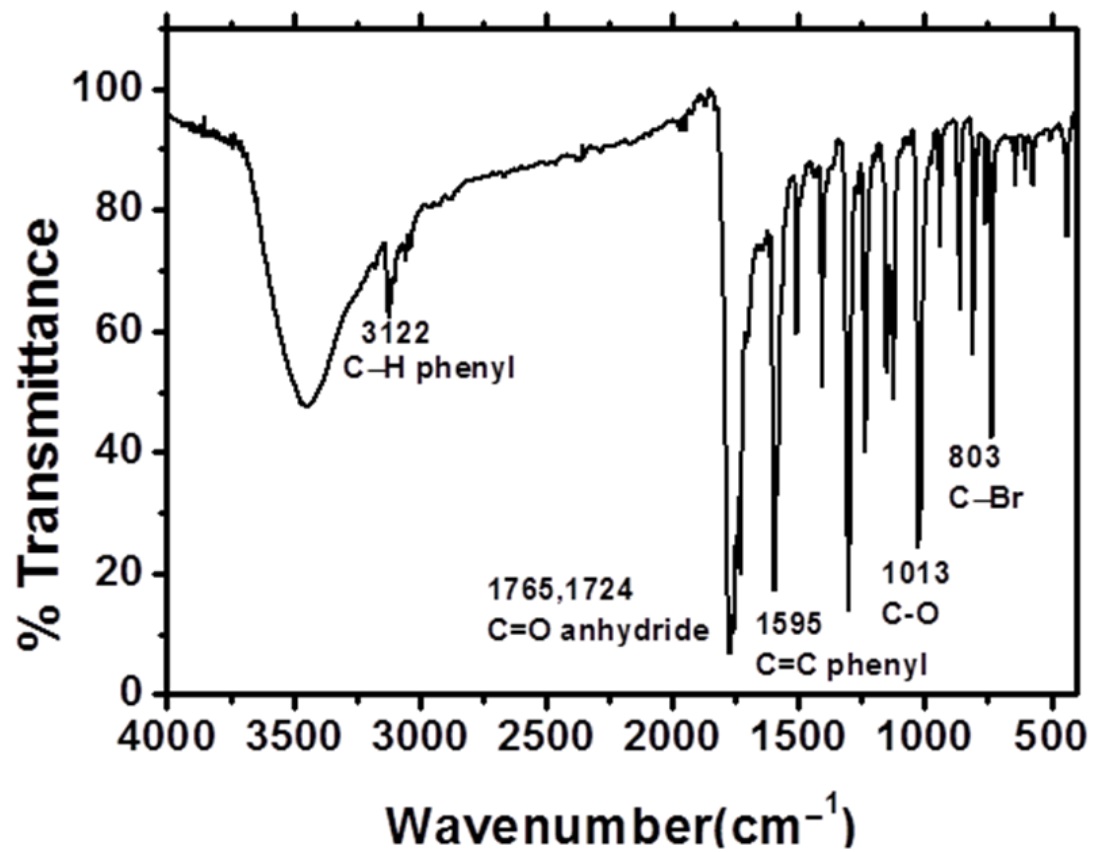


Figure 4.3: FTIR spectrum of Br-PDA

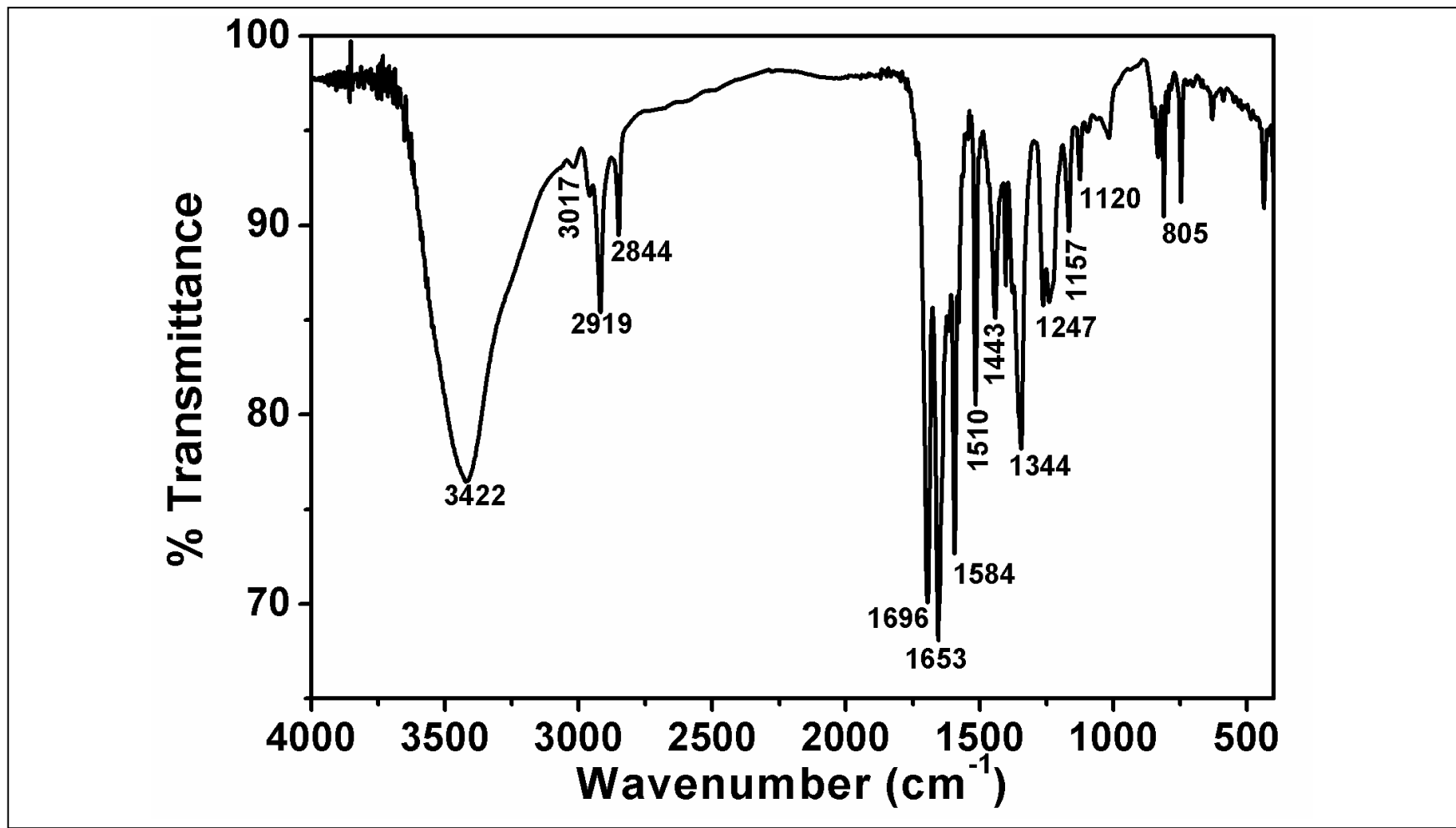


Figure 4.4: FTIR spectrum of Ty-B-PDI

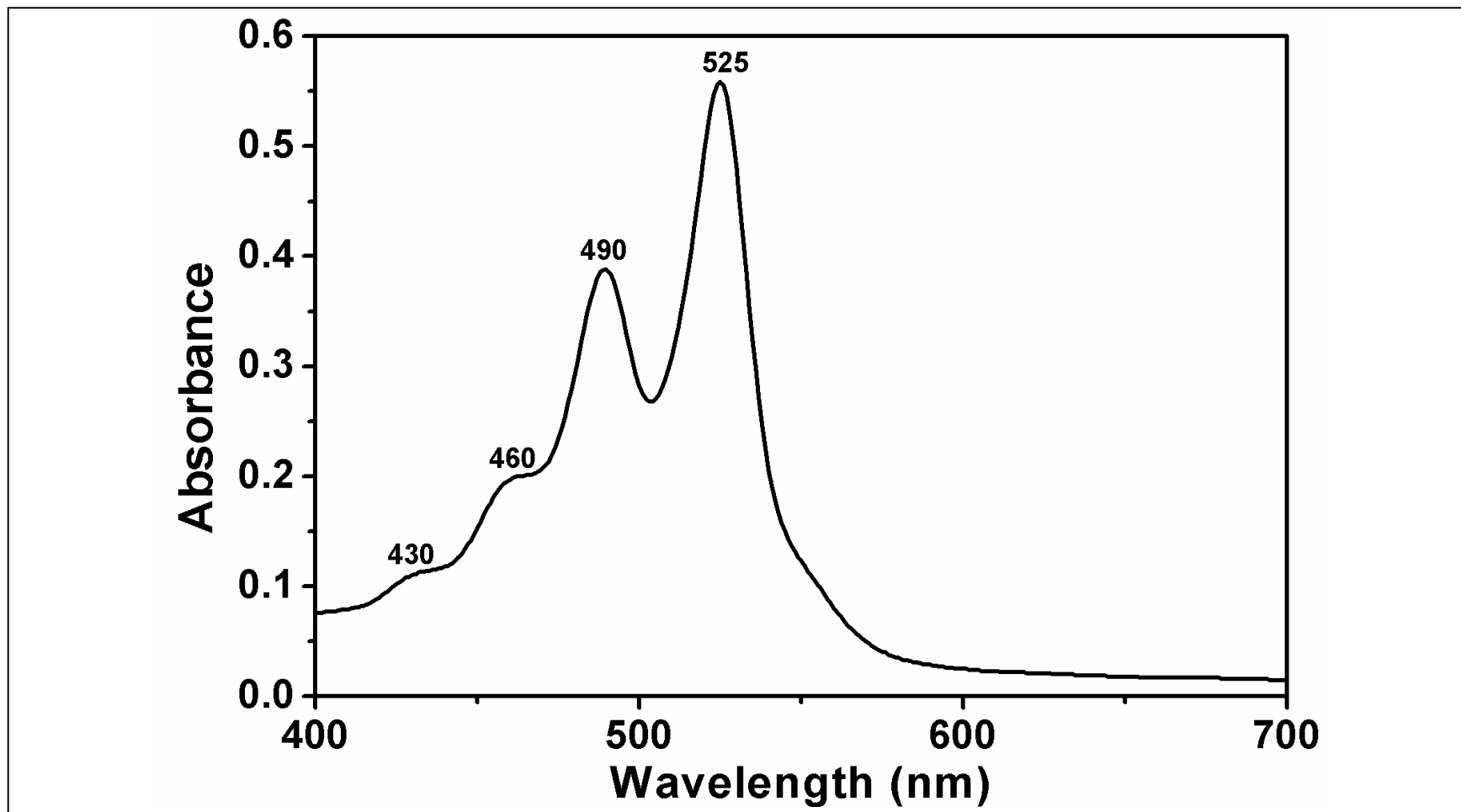


Figure 4.5: Absorption spectrum of Ty-B-PDI in DMF

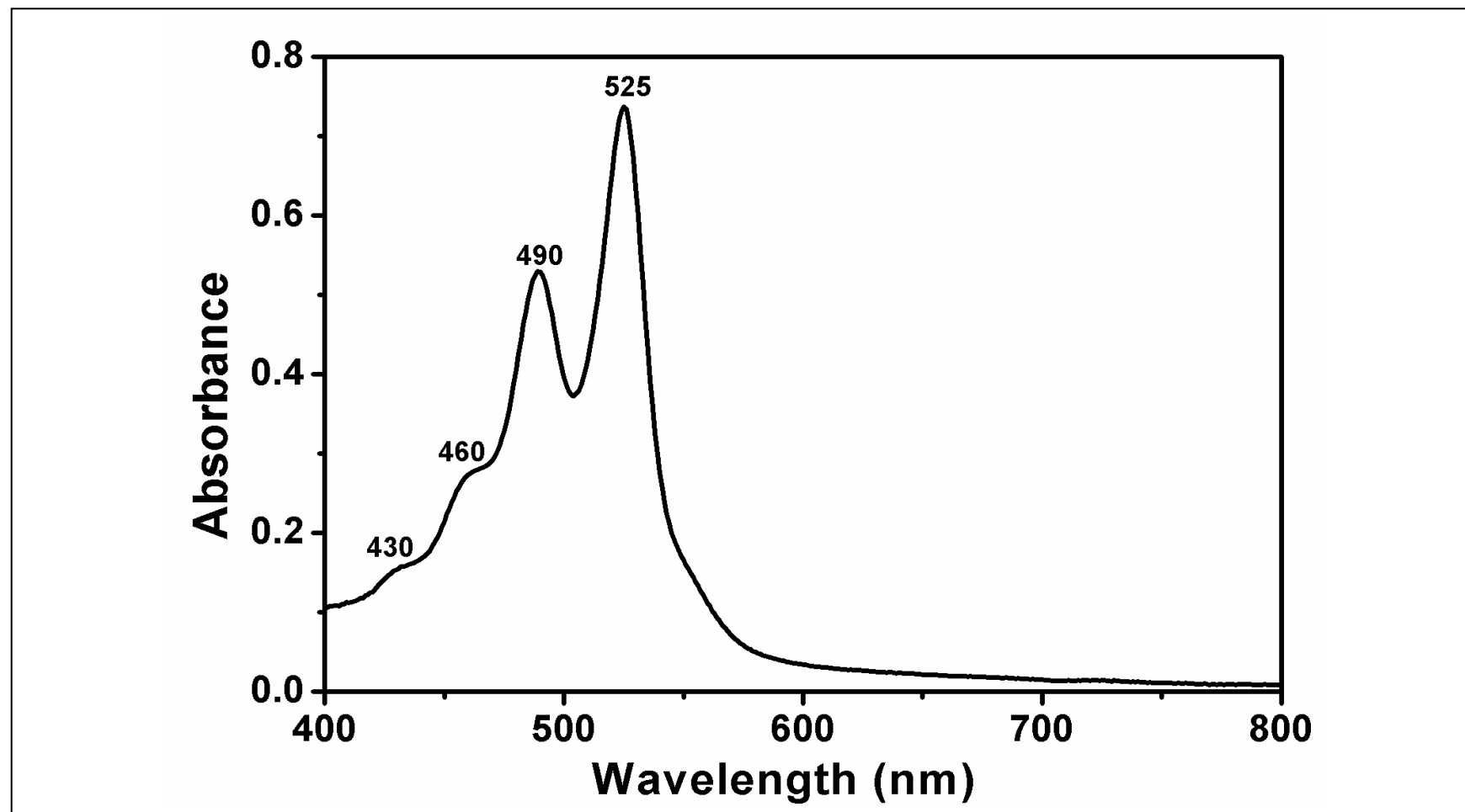


Figure 4.6: Absorption spectrum of Ty-B-PDI in DMF after microfiltration (0.2 μm)

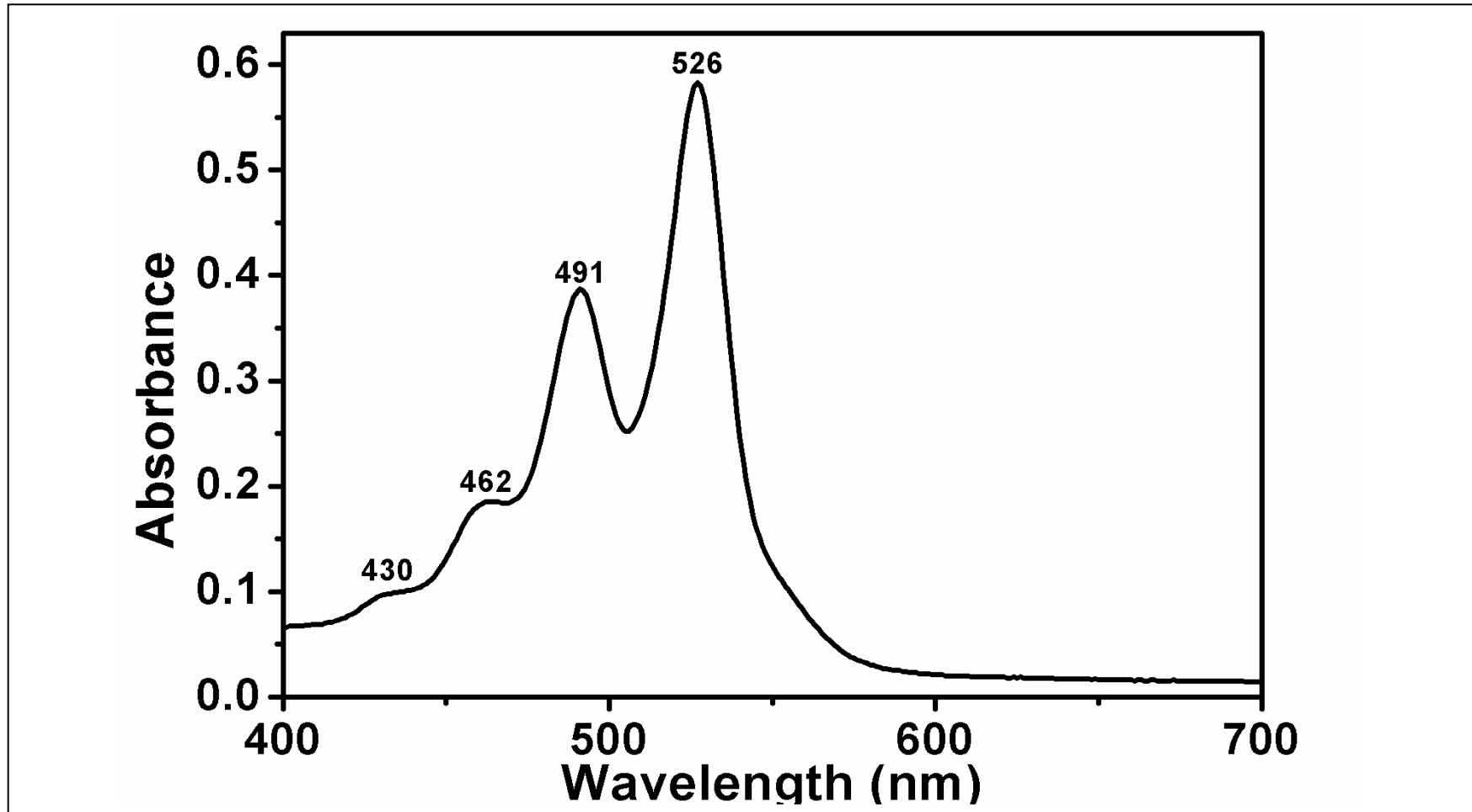


Figure 4.7: Absorption spectrum of Ty-B-PDI in NMP

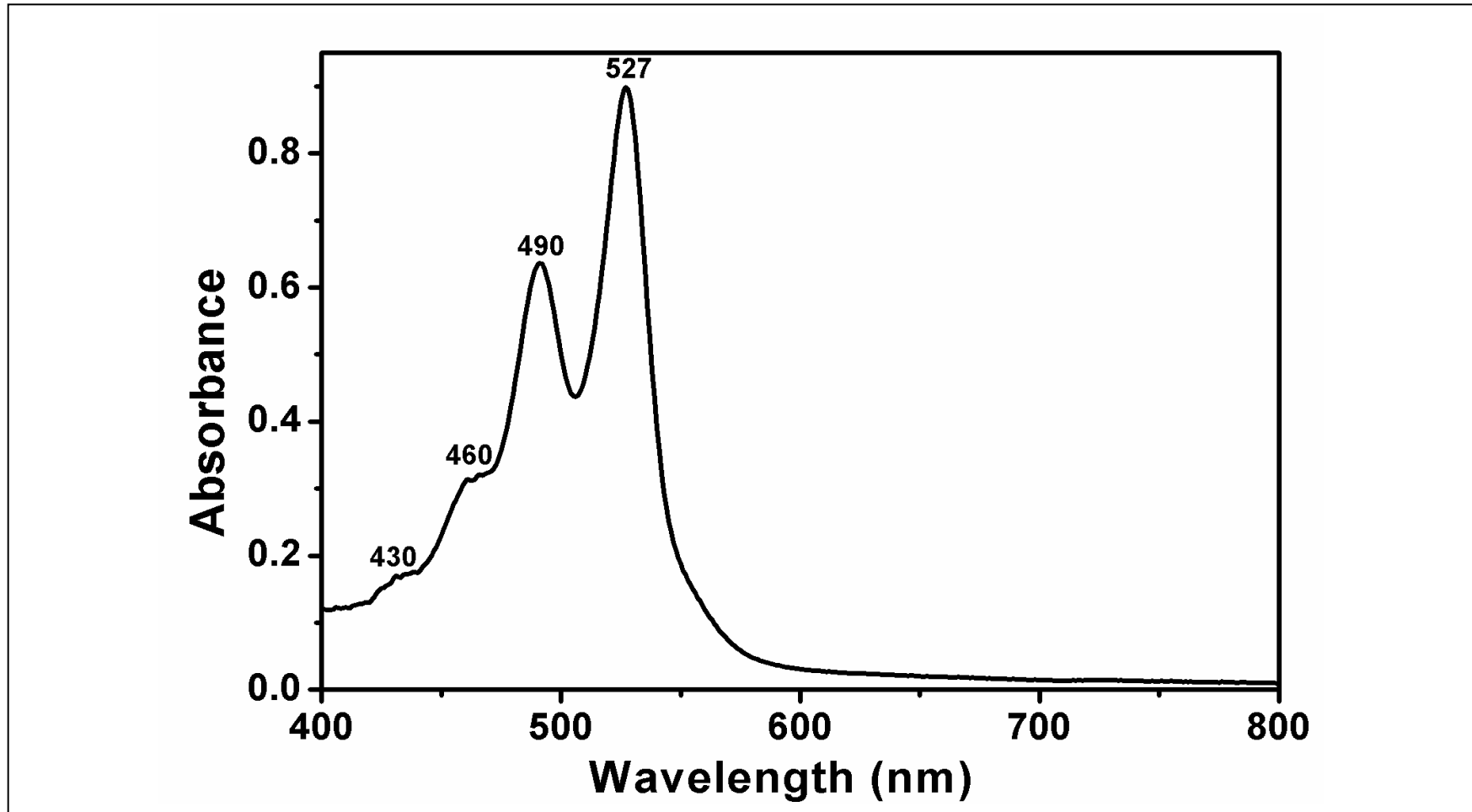


Figure 4.8: Absorption spectrum of Ty-B-PDI in NMP after microfiltration (0.2 μm)

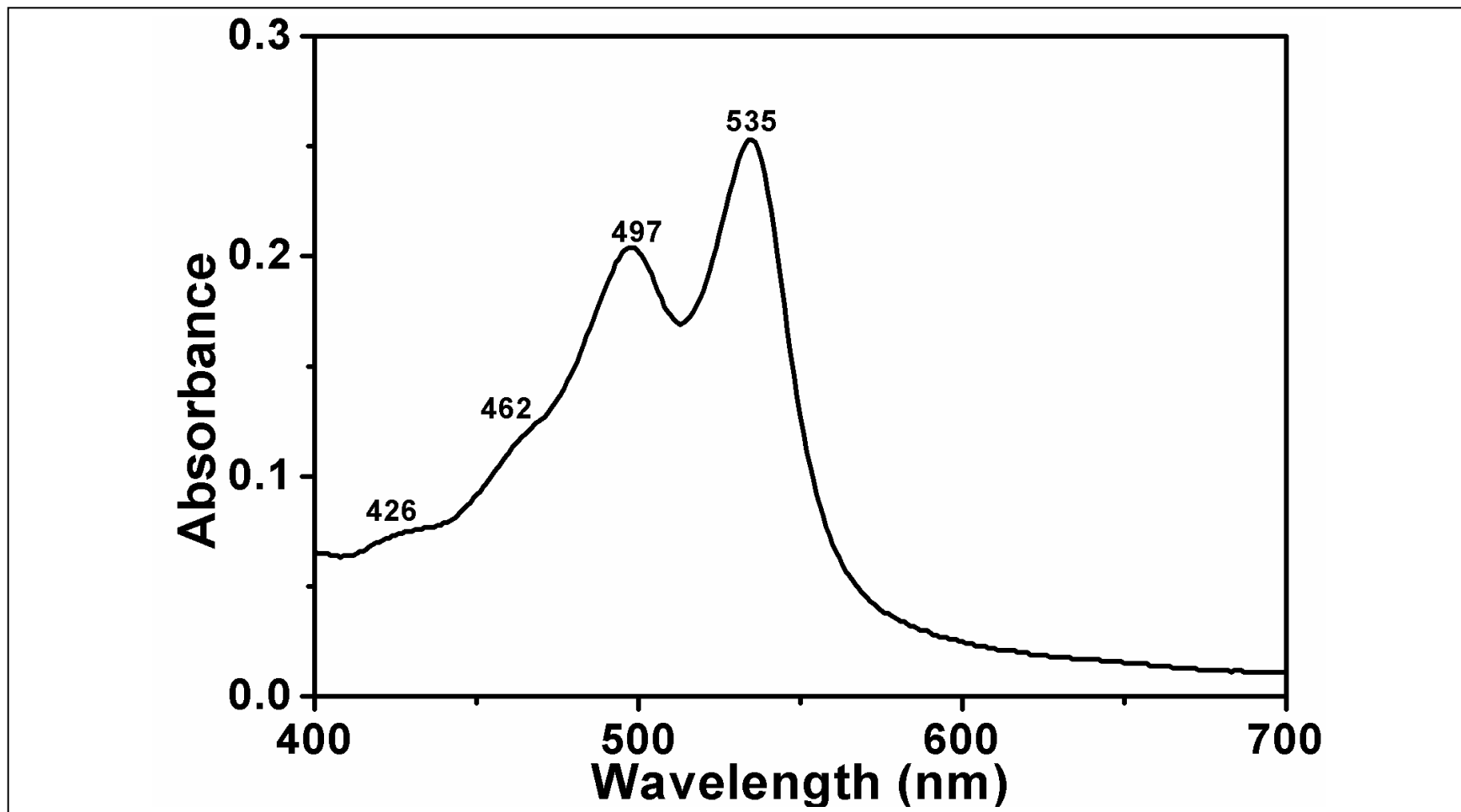


Figure 4.9: Absorption spectrum of Ty-B-PDI in TFA

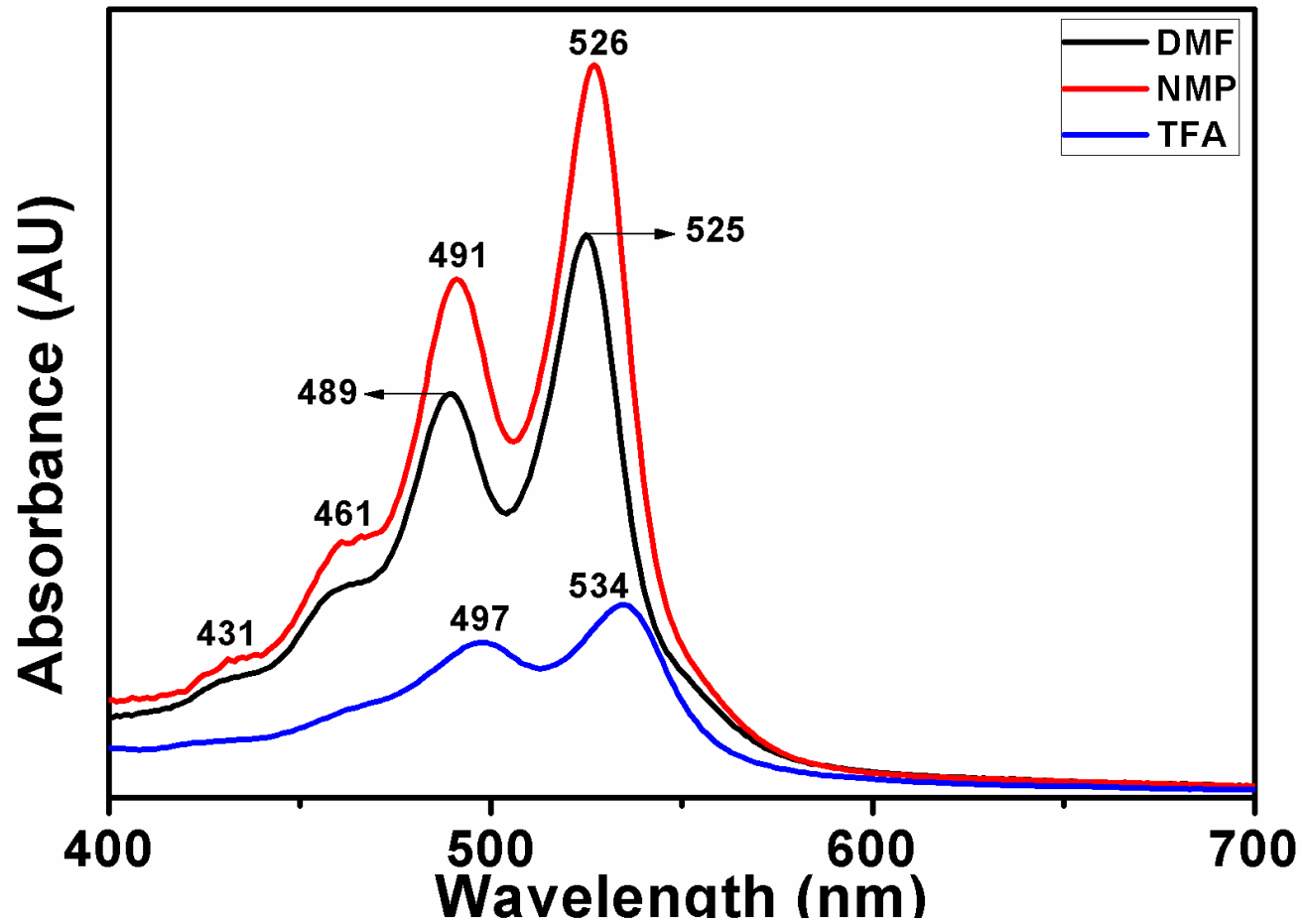


Figure 4.10: Absorption spectra of Ty-B-PDI in DMF, NMP and TFA

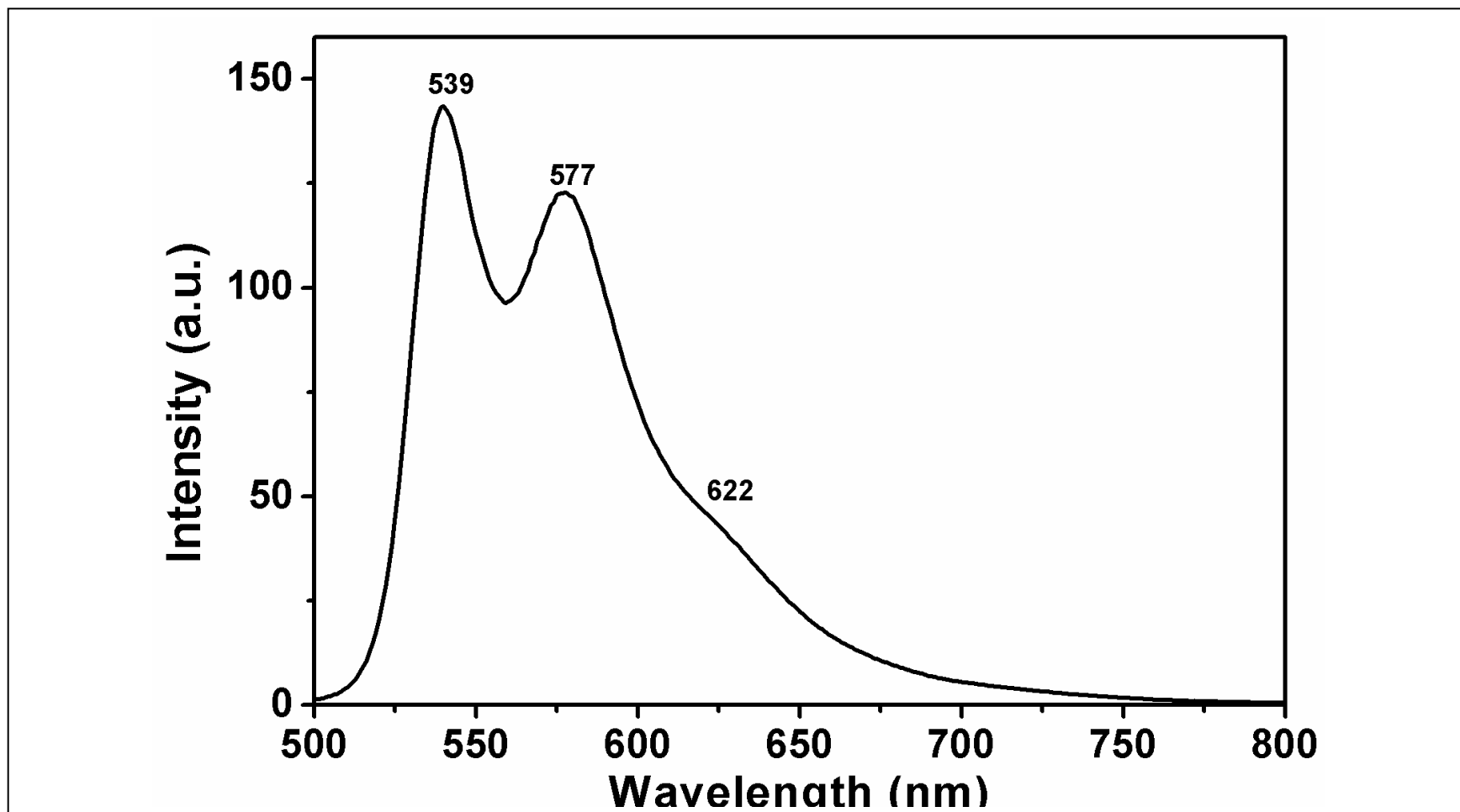


Figure 4.11: Emission spectrum of Ty-B-PDI in DMF

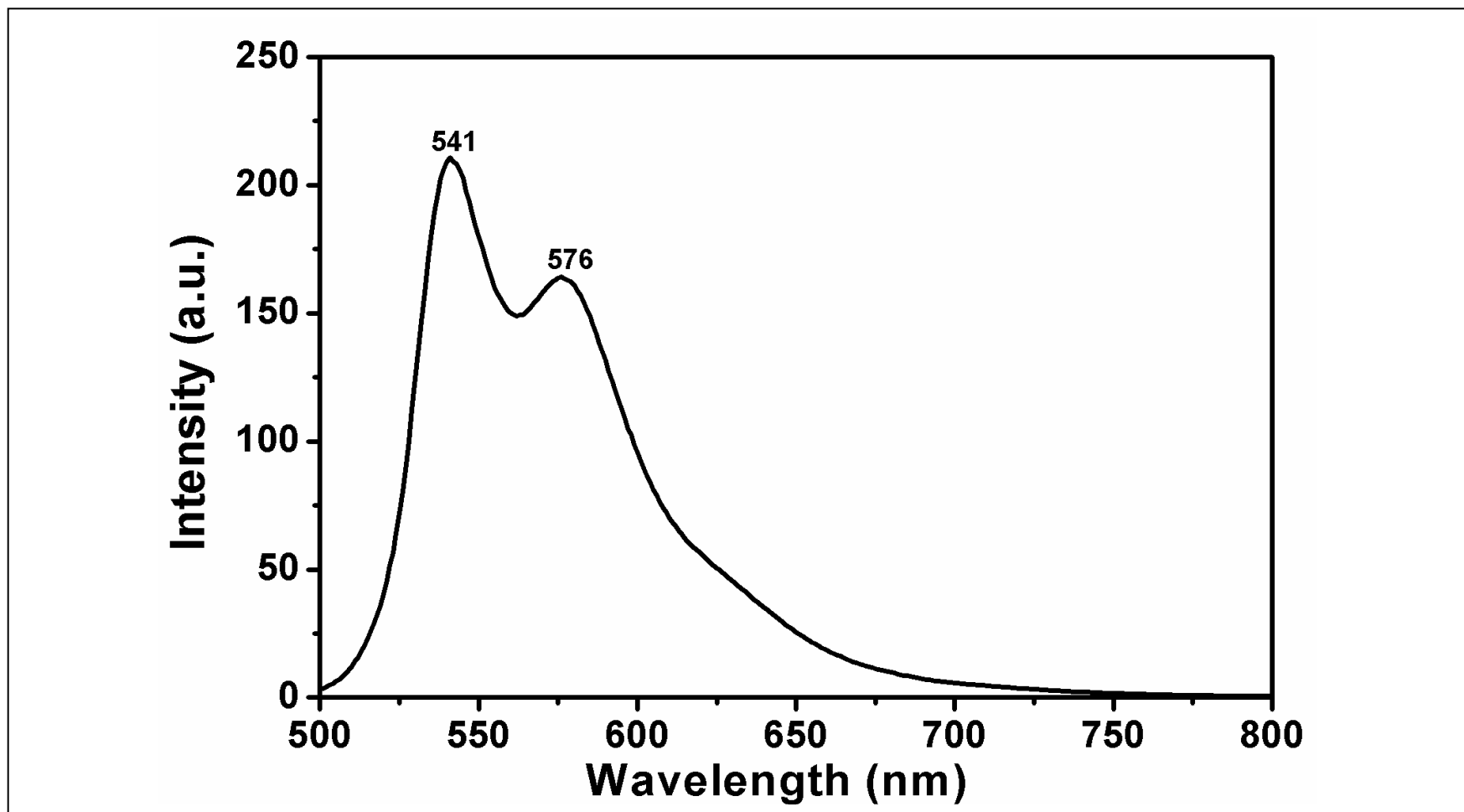


Figure 4.12: Emission spectrum of Ty-B-PDI in DMF after microfiltration (0.2 μm)

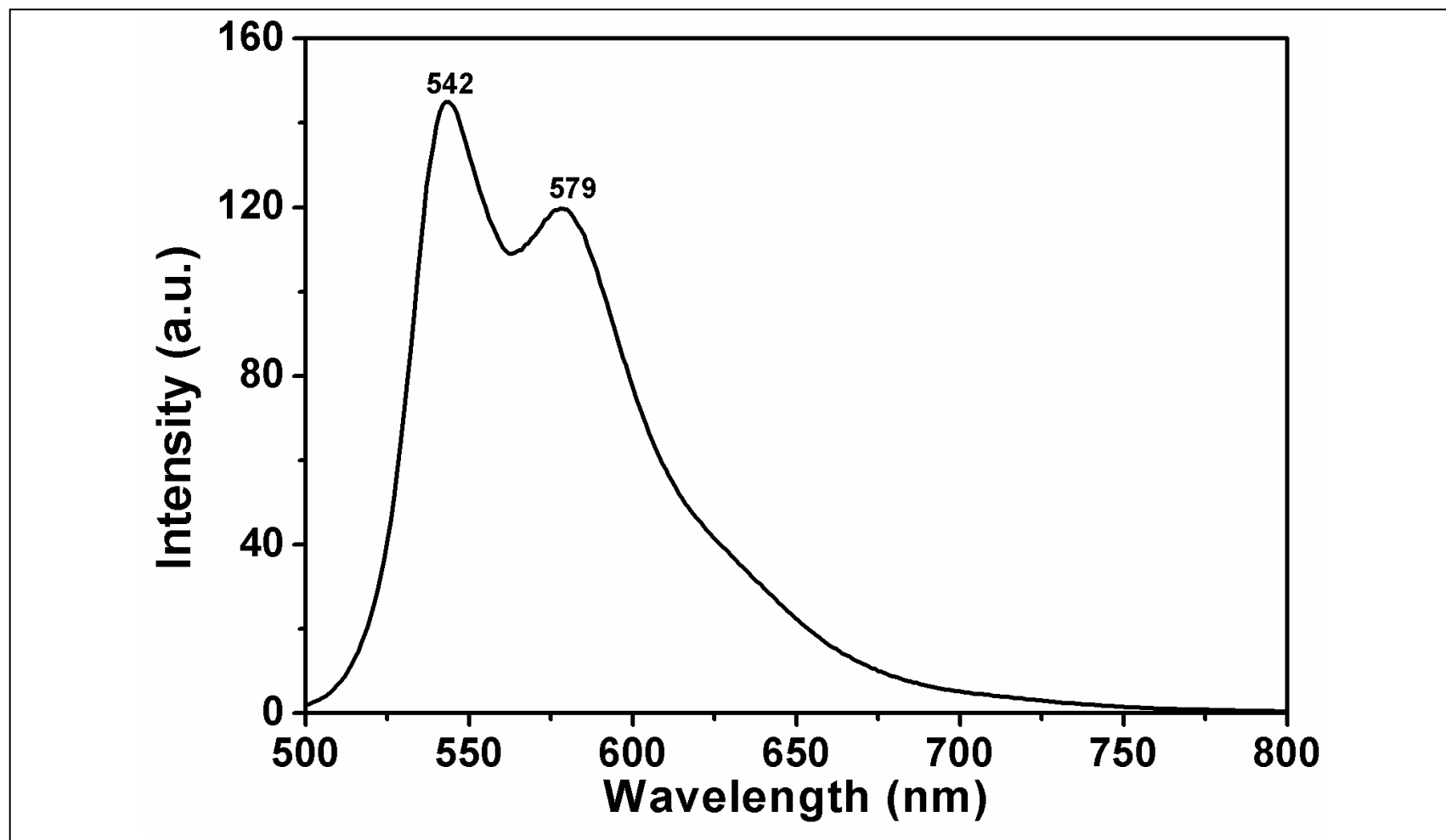


Figure 4.13: Emission spectrum of Ty-B-PDI in NMP

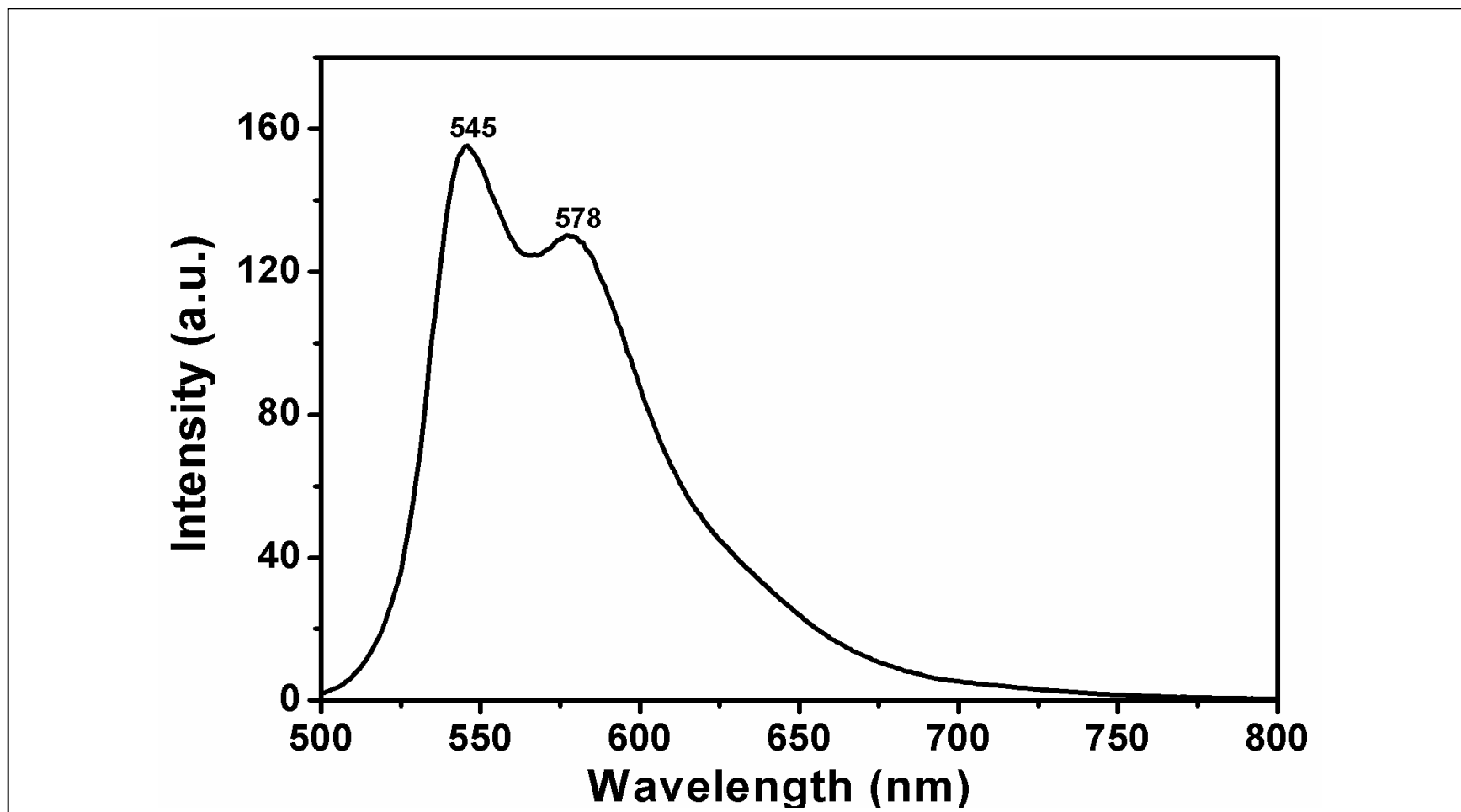


Figure 4.14: Emission spectrum of Ty-B-PDI in NMP after microfiltration (0.2µm)

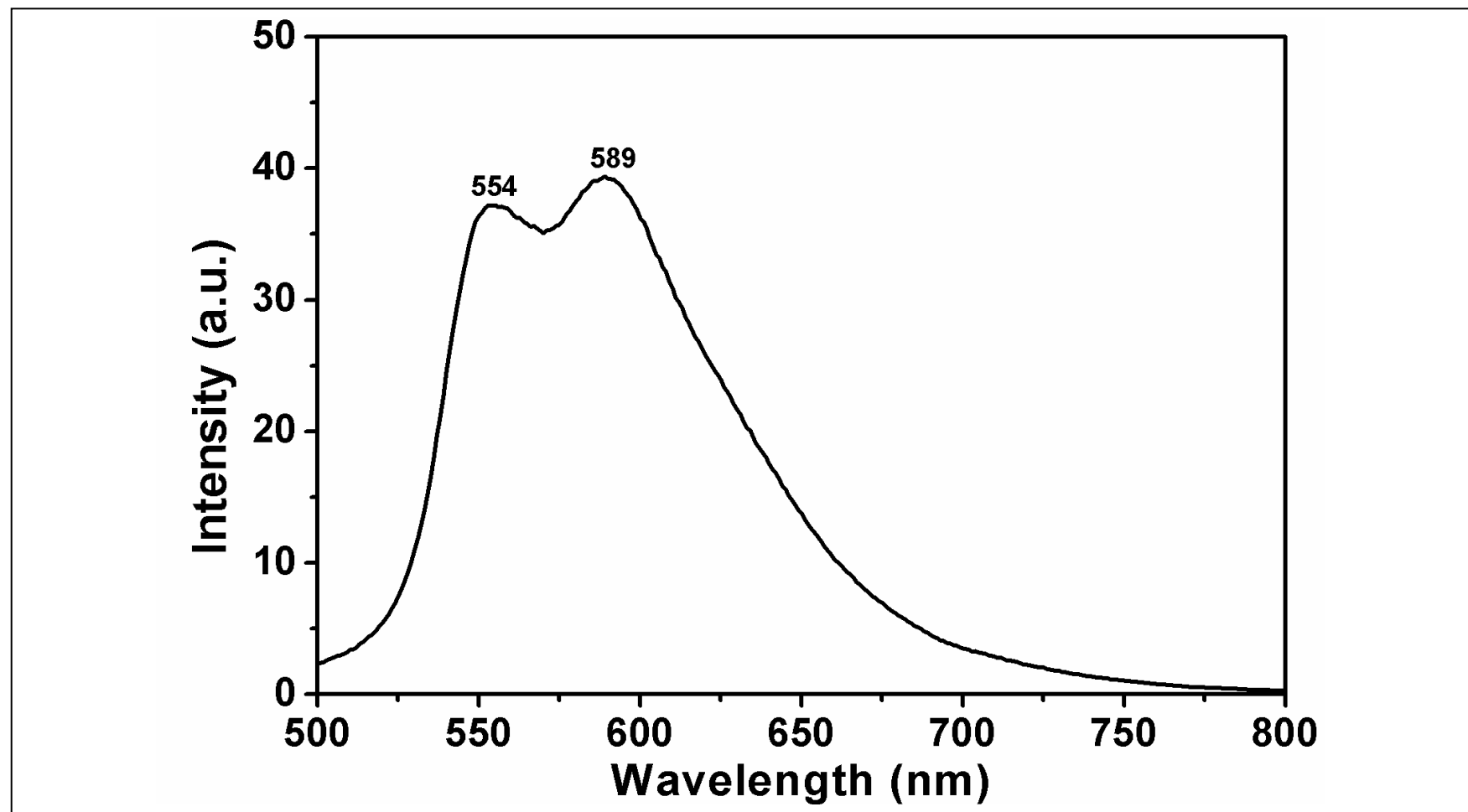


Figure 4.15: Emission spectrum of Ty-B-PDI in TFA

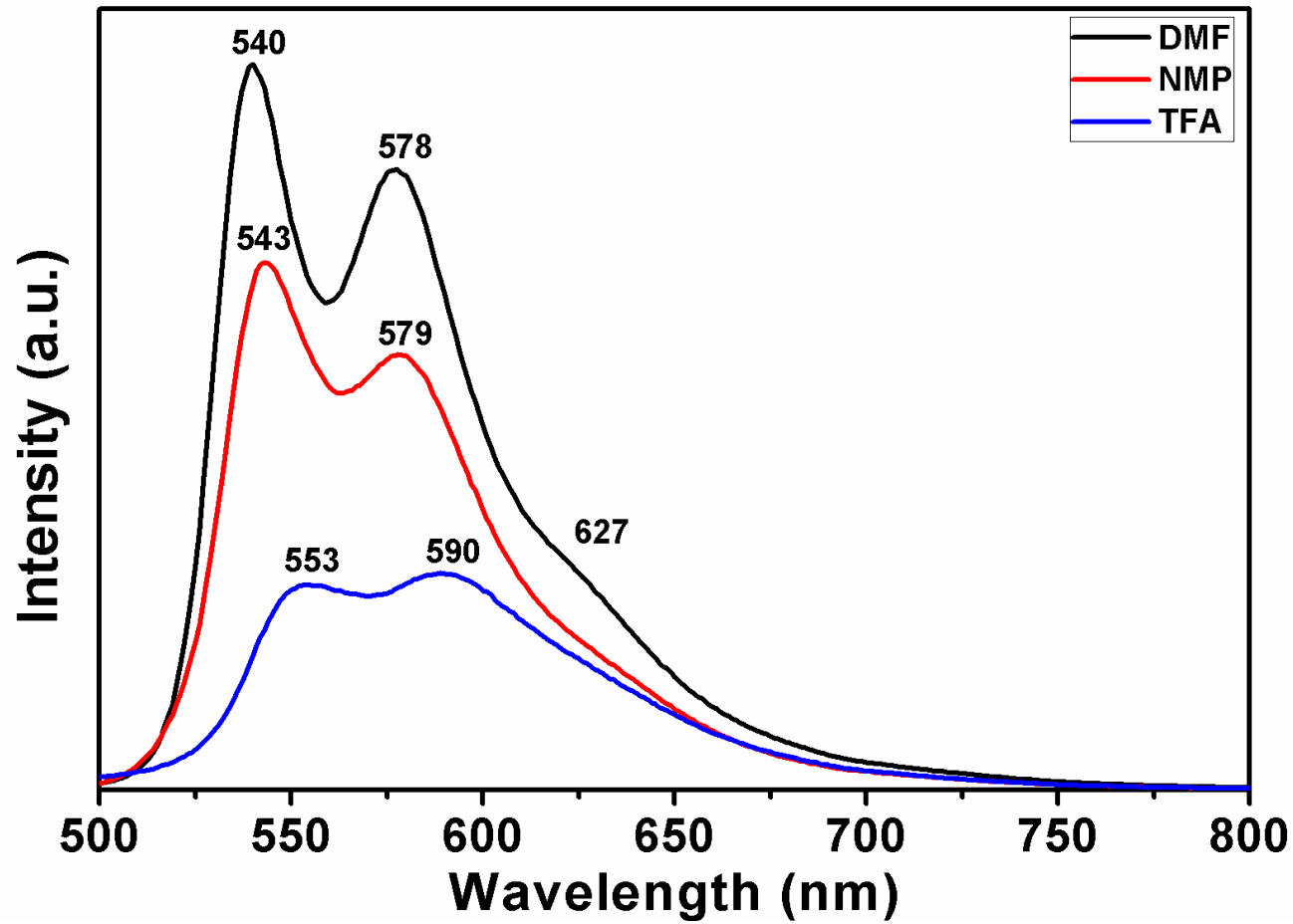


Figure 4.16: Emission spectra of Ty-B-Pb DI in DMF, NMP and TFA

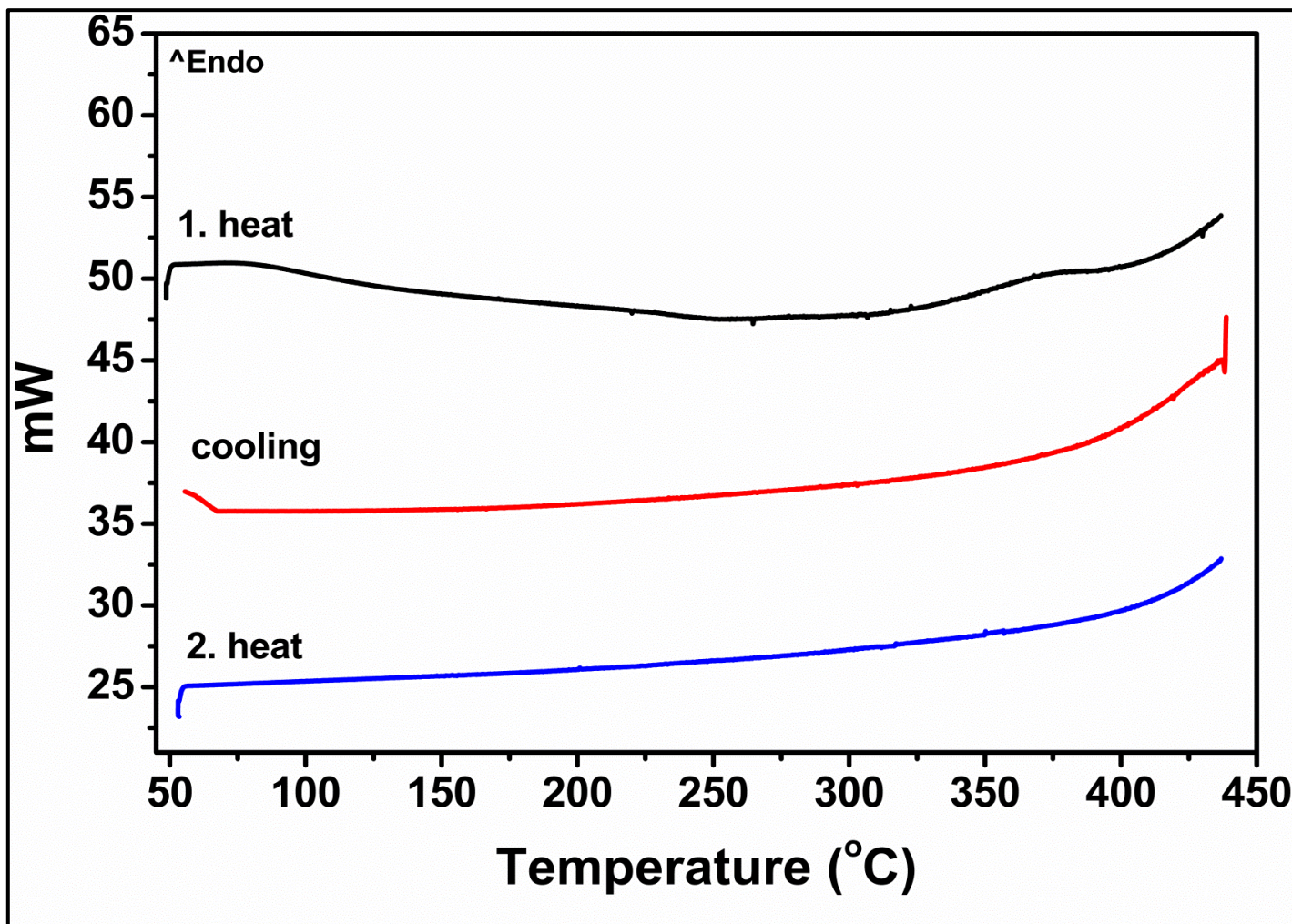


Figure 4.17: DSC Curve of Ty-B-PDI at the heating 10⁰C/min in nitrogen.

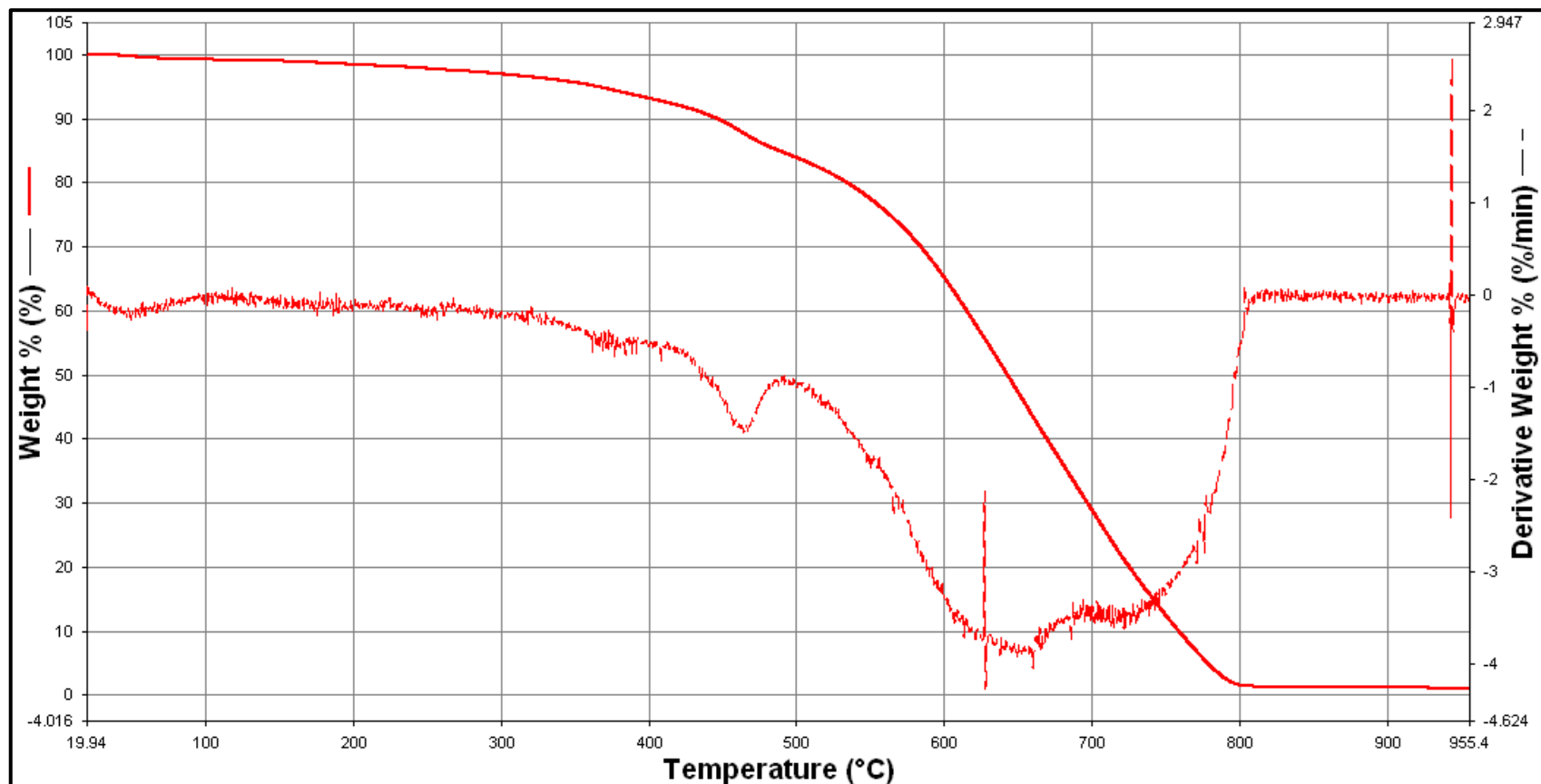


Figure 4.18: TGA thermogram of Ty-B-PDI at heating rate of 10^0 C /min in oxygen

Chapter 5

RESULTS AND DISCUSSION

5.1 Synthesis and Characterization

Bay and imide substitutions of a compound were prepared according to the synthetic routes shown in Scheme 3.1 and Scheme 3.2, respectively. The brominated perylene tetracarboxylic dianhydride was directly converted to an intermediate product via condensation with 4-(2-aminoethyl) phenol at 150 °C for 24 hrs. The reaction was further continuous for 4 hrs at 120 °C, for 3 hrs at 150 °C, for 2hrs at 180 °C and for 1 hr at 200 °C under argon atmosphere. The structure of the compound was characterized by IR, UV-vis, DSC, TGA and elemental analysis. The results have actually proved the predicted chemical structure of the compound.

The characterization of bending and stretching Absorption of functional group in FT-IR Spectrum of synthesized compound was put across.

All IR Spectrum of Tyramine in fig.4.2 shows the characteristic Absorption bands at 3340 cm^{-1} (N-H stretch), 3279 cm^{-1} (Ar C-H stretch), 2935 and 2867 cm^{-1} (aliphatic C-H stretch) 1592 and 1517 cm^{-1} (C=C stretch), 1465 cm^{-1} (C-N stretch), 1112 cm^{-1} (C-O stretch) and 821 cm^{-1} (C-H bend).

IR spectrum of the Br-PDA was consistent with the assigned structures as shown in Fig.4.3 (Ar C-H stretch) 3122 cm^{-1} , anhydride C=O stretch at 1765 cm^{-1} and 1724

cm^{-1} , (C=C stretch) at 1595cm^{-1} , (C–O stretch) at 1013cm^{-1} , (C–Br) at 803cm^{-1} proved the structure of Br-PDA.

The IR Spectrum of Ty-B-PDI in Fig. 4.4, has also shown the characteristic bands at 3422cm^{-1} (O-H and N-H stretch); 3017 cm^{-1} (Ar C-H stretch); 2919cm^{-1} and 2844 cm^{-1} (aliphatic C-H stretch); 1696 cm^{-1} and 1653cm^{-1} (imide C=O); 1584cm^{-1} and 1510cm^{-1} (C=C stretch); 1344cm^{-1} (C-N stretch); 1157cm^{-1} (C-O stretch) and 805cm^{-1} (C-H bend), confirmed the structure of Ty-B-PDI.

Following the IR spectrum of Br-PDA the characteristic bands of the anhydride C=O stretch (1762 cm^{-1}) had vanished and were substituted by imide C=O stretch (1696 and 1653 cm^{-1}). Similarly, the characteristic band of the C–O–C stretching (1024 cm^{-1}) had disappeared and was replaced by C–N stretch (1344cm^{-1}).

Highly soluble PDI is of important for process ability and preparation of thin film that can be used in organic electronics. The improved solubility of PDI derivatives have originated from the bulky substituent on core area and imide position of perylene chromophore. However the presence of tyramine also known as 4-(2-aminoethyl) phenol on the synthesized product have shown a good solubility in dipolar aprotic solvents and also little or partially soluble in polar protic solvents as in (Table 5.1). The partial solubility of the product in polar protic solvents could be due to the presence of hydrogen bonding

Table 5.1: The solubility properties of Ty-B-PD1 in different solvents

Solvents	Solubility	Color
DMF	(+ +)	Red
NMP	(+ +)	Red
DMSO	(- +)	Red
<i>m</i>-CRESOL	(- +)	Red
TFA	(- +)*	Pale red
ACETONE	(- +)*	Pale orange
DCM	(- -)	Colorless
TCE	(- -)	Colorless
CCl₄	(- -)	Colorless

CCl₄; Tetrachloromethane, DMF; Dimethylformamide, DMSO; Dimethyl Sulfoxide, DCM; Dichloromethane, NMP; N-methylpyrrolidinone, TCE; Trichloroethylene, TFA; Trifluoroacetic acid, (+ +): Soluble at room temperature; (- +): Partly soluble at room temperature; * Solubility increased upon heating at 60 °C.

5.2 Absorption and Fluorescence Properties

Optical properties of Ty-B-PDI were investigated through UV-vis absorption and emission spectra. The measured data obtained from UV-vis absorption and emission spectra in different solvents are used in calculating of various physical parameters as shown in table 4.1- 4.9, respectively. Significantly, appreciable solubility of the compound and the polarity of the solvent were considered when taking the measurements.

However, the absorption spectra of the compound in various solvents were presented in fig. 4.5 – 4.10. Figure 4.6 indicates the absorption spectrum of Ty-B-PDI in dipolar aprotic solvent DMF with the characteristic bands at 525, 490 and 460 nm, respectively. These characteristic bands of absorption intensities are due to

intermolecular charge transfer and $\pi \rightarrow \pi^*$ electronic transitions from ground state to excited states, representing the $0 \rightarrow 0$, $0 \rightarrow 1$, and $0 \rightarrow 2$, respectively.

The UV spectrum of Ty-B-PDI in Fig. 4.8 shows three characteristic peaks with maximum absorption of 527 nm in NMP. Interestingly, the absorption spectrum a compound has shown the characteristic peaks at 527, 490 and 460 nm with a shoulder peak at 430 nm after microfiltration. This additional shoulder peak for Ty-B-PDI in NMP is likely due to aggregation of Ty-B-PDI molecule in solution. It is also observed that there is no any significant different between absorption spectra of Ty-B-PDI in DMF and NMP.

The UV spectrum of Ty-B-PDI in Fig. 4.9 shows the traditional characteristic absorption bands at 535, 497, and 462 nm, with a shoulder peak of 426nm respectively. Notably, in polar protic solvent TFA, the compound exhibit diminished absorption bands with red shifted spectra due to the increase in solvent polarity which attributed to possible hydrogen bonding, also the broadest wavelength of absorption peak of the compound in polar solvent TFA is an indication of nonappearance of a strong charge transfer in a ground state.

The emission spectra of all Ty-B-PDI were taken at $\lambda_{exc} = 485$ nm excitation wavelength as presented in Fig. 4.11 – 4.16. The characteristics emission bands of Ty-B-PDI in different solvents are observed at 541 and 547 nm for DMF, 545 and 578 nm for NMP and 554 nm, 589 nm for TFA. Considerable red shift emission observed in TFA comparing to the rest of the solvents were identified from emission spectra of Ty-B-PDI in difference solvents Fig.4.16.

The red shift in polar aprotic indicate the better solvation of the excited state than the polar ground state of Ty-B-PDI. Fluorescence quantum yields (Φ_f) of the compound are measured in different solvents and were presented in Table 4.2. Essentially, the Ty-B-PDI has displayed low fluorescence quantum yield (Φ_f) in NMP. Meanwhile, the poor fluorescence quantum yields in different solvents are attributed to the re-absorption of emitted photons and the self-quenching because of the intra and intermolecular interactions.

5.3 Mass Spectra Analysis

The MS analysis of Ty-B-PDI was not successfully captured due to the poor solubility of the compound.

5.4 Thermal Stability

Thermal properties of Ty-B-PDI were investigated by DSC (differential scanning calorimetry) at 10 K min^{-1} in Fig. 4.17 and TGA (thermogravimetry) at 5 K min^{-1} in Fig 4.18. Ty-B-PDI compound did not show any glass transition temperature in DSC run. The TGA curve displayed high starting decomposition temperature T_d , which proved thermal stability property of the compound. The compound was also stable at $450 \text{ }^\circ\text{C}$. Ty-B-PDI experienced a rapid weight loss of 10 % occurred at $450 \text{ }^\circ\text{C}$ and $530 \text{ }^\circ\text{C}$. When Ty-B-PDI compound was heated up to $800 \text{ }^\circ\text{C}$, 98 % of initial weight were lost and 2 % char yield was observed.

Chapter6

CONCLUSION

Perylene dyes have been favorably synthesized from reactants involving 1,7-dibromoperylene -3,4,9,10-tetracarboxylic dianhydride (Br-PDA) and 4-(2-aminoethyl)phenol. The structure and the properties of the Ty-B-PDI compound have been well investigated and characterized by FTIR, UV-vis, MS, DSC, TGA, and elemental analysis.

The compound showed a good solubility in polar aprotic solvent and partial solubility in polar protic solvents due to the presence of intermolecular hydrogen bonding in the substituent. However, the compound was not soluble in non-polar solvents. Ty-B-PDI achieved high thermal stability at $>450^{\circ}\text{C}$ where it is possible to use it in some devices as temperature and heat resistant compound.

The absorption spectrum of Ty-B-PDI in TFA show a broad and red shifted absorption spectrum which indicating hydrogen bonding. The compound recorded high absorption ability in DMF and NMP; hence the high absorptivity of a chromophore is an attractive property toward photovoltaic materials.

The emission spectra of the core substituted Perylene diimide in various solvents before and after microfiltration were also reported. All the emission spectra show two emission peaks of $0 \rightarrow 0$ and $0 \rightarrow 1$ transitions of perylene chromophore which

where mirror images of Absorption spectra. Fluorescence quantum yield value of Ty-B-PDI is low in NMP and DMF.

On balance, the analysis results obtained from the research could bring about further development in photovoltaic applications.

REFERENCES

- [1] Haung, C., Barlow, S., & Marder, S. R. (2011). Perylene-3,4,9,10-tetracarboxylic acid diimides synthesis, physical properties, and use in Organic Electronics. *Journal of Organic Chemistry*, 76, 2386-2407.
- [2] Li, C., & Wonneberger, H. (2012). Perylene imides for Organic Photovoltaics Yesterday, Today, and Tomorrow. *Advanced Materials*, 24, 613-636.
- [3] Würthner, F. (2004). Perylene bisimide dyes as versatile building blocks for functional supramolecular architectures. *Chemical communications*, 14, 1564-1579.
- [4] Greene, M., Faulkner, E. B., Schwartz, R., & Eds. J. (2009). Wiley-VCH: Weinheim. *High Performance Pigments*. John Wiley & Sons.
- [5] Kardos, M. (1913). Deutsches Reichsoatent no 276, 357.
- [6] Faulted, E. B. (2009). Wiley-VCH Weinheim. *High Performance Pigments*.
- [7] Icil, H., & Icli, S. (1997). Synthesis and properties of a new photostable polymer; perylene-3,4,9,10-tetracarboxylic acid-bis-N-N-dodecylpolyimide. *Journal of polymer science*, 35, 2137-2142.

- [8] Perlstin, J. (1994). Molecular self-assembly. 3. Quantitative Predictions for the packing Geometry of Perylene dicarboximide translation aggregates and the effects of flexible end groups. Implications for monolayers and three-dimensional crystal structure predictions. *Chemistry of materials*, 6, 319-326.
- [9] Lv, A., Puniredd, S. R., Zhang, J., Li, Z., Zhu, H., Jiang, W., Dong, H., He, Y., jiang, L., & Li, Y. (2012). High mobility,air Stable, Organic Single Crystal Transistors of an n-type diperylene bisimide. *Advance material*, 24, 2626-2630.
- [10] Jones, B. A., Facchetti, A., Wasielewsk, M. R., & Marks, T. J. (2007). Turning Orbital Energetics in arylene diimide semiconductors. Material Design for ambient Stability of n-type charge transport. *Journal of American Chemical Society*, 129, 15259-15278.
- [11] Ranke, P., Bleyl, I., Simmerer, J., Haarer, D., Bacher, A., & Schmitdt, H. W. (1997). Electroluminescence and electron transport in a perylene dye. *Applied Physics Letters*, 71, 1332-1334.
- [12] Bffreau, J., Leroy-Lhez, S., Anh, N. V., Williams, R. M., & Hudhomme, P. (200). Fullerene C₆₀-Perylene-3,4,9,10-bis(dicarboximide) light –harvesting dyads Spacer-length and bay-Substituted Effects on intermolecular singlet and triplet Energy transfer. *Chemistry European Journal*, 14, 4974-4992.
- [13] Weiss, E. A., Ahrens, M. J., Sinks, L. E., Gusev, A. V., & Wasielewski, M. A. R. (2004). Making a molecular wire; charge and spin transport through paraphenylene oligomers. *Journal of American Society*, 126, 5577-5584.

- [14] Guo, X., Zhang, D., & Zhu, D. (2004). Logic control of the fluorescence of a new dyad, spiropyran-perylene diimide spiropyran, with light, ferric ion and proton: construction of a new three-input AND logic gate. *Advance Materials*, 16, 125-130.
- [15] He, X., Liu, H., Li, Y., Wang, S., Xiao, J., Xu, X., & Zhu, D. (2005). Gold Nanoparticle-Based Fluorometric and Colorimetric Sensing of Copper(II) Ions. *Advanced Materials*, 17, 281–2815.
- [16] Wurhner, F. (2006). bay-substituted perylene bisimides Twisted fluorophores for supramolecular chemistry. *Pure Applied Chemistry*, 78, 2341- 2349.
- [17] Lin, L., Geng, H., Shuai, Z., & Luo, Y. (2012). Theoretical insights into the charge transport in perylene diimides based n-type organic semiconductors. *Organic electronics*, 13(11), 2763-2772.
- [18] Guldi, D. M., Luo, C., Prato, M., Troisi, F., Zerbetto, M., Scheloske, E., Diwtel, B. W., & Hirsch, A. (2001). parallel (face to face) alingement of electronorientation in electron transfer. *Journal of American Chemical Society*, 123, 9166-9167.
- [19] Wenger, O. S. (2011). How donor-bridge-acceptor Energetics influence Electron tunneling dynamics and their distance dependences. *Account of Chemical Research*, 44, 25.
- [20] Jones, B. A., Ahrens, M. J., Yaon, M. H., Facchetti, A., Marks, T. J., &

Wasielewski, M. R. (2004). High-mobility air-stable n-type semiconductors with processing versatility: dicyanoperylene-3, 4, 9, 10-bis(dicarboximides). *Chemie International Edition*, 43, 6363.

[21] Chen, Z. J., Debiji, M. G., Debaerdemaeker, T., Osswald, P., & Würthner, F. (2004). Tetrachloro-substituted perylene diimide dye as promising n-type organic semiconductors: studies on structural, electrochemical and charge transport properties. *Chemical Physical Chemistry*, 5, 137-140.

[22] Katz, H. E., Lovinger, A. J., Johnson, J., Kloc, C., Siegrist, T., Li, V., & Lin, Y. Y. (2000). Dodabalapur, A soluble and air-stable organic semiconductor with high electron mobility, nature. *Advanced Materials*, 404, 478-481.

[23] Schmidt, R., Ling, M. M., Oh, J. H., Winkler, M., Konemann, M., Bao, Z. N., & Würthner, F. (2007). Core-fluorinated perylene bisimide dyes: air stable n-channel organic semiconductors for thin film transistor with exceptionally high on to-off current ratios. *Advanced Materials*, 19, 3692- 3695.

[24] Oh, J. H., Suraru, S. L., Lee, V., Könnemann, M., Höffken, H. W., Röger, C., Schmidt, R., Chung, Y., Chen, V., Würthner, F., & Bao, V. (2010). High performance air stable n-type organic transistors based on corechlorinated naphthalene tetracarboxylic diimides. *Advanced Functional Materials*, 20, 2148-2156.

[25] Herbst, W., Hunger, K., & Weinheim (1997). Industrial Organic Pigments. *Second Completely Revised Edition*.

- [26] Icil, H. (1998). Energy Transfer Studies with Perylene bis-diimide derivatives. *Spectroscopy Letters*, 31, 747-755.
- [27] Bodpati, J. B., & Icil, H. (2008). Highly Soluble Perylene diimide dyes combining perylene and Hexa (Ethylene Glycol) unit: Synthesis, haracterization, optical and Electrochemical Properties. *Dyes and Pigments*, 79, 224-235.
- [28] Masono, T., & Nagao, Y. (1984). Synthesis and properties of N-alkyl-N-aryl-3,4,9,10-perylene bis(dicarboxyimide). *Dyes and Pigments*, 5, 171.
- [29] Markle, V., Rademacher, A., & Langhals, H. (1982). Soluble Perylene Fluorescent Dyes with high photostability. *Chemische Berichte-recueil*, 117, 2927.
- [30] Lai, G., Zhang, Y., Cai, L., Qiu, H., & Shen, Y., & Xu, Z. (2008). Highly soluble perylene tetracarboxylic diimides and tetrathiafulvalene-perylene tetracarboxylicdiimide-tetrathiafulvalene triads. *Journal of photochemistry and Photobiology A: Chemistry*, 200, 334-345.
- [31] Fan, L., Xu, Y., & Tian, H. (2005). 1,6-Disubtitued perylene bisimides: concise Synthesis and characterization as near-infrared fluorescence dyes. *Tetrahedron Letters*, 46, 4443-4447.
- [32] Jones, B. A., Facchetti, A., Wasielewsk, M. R., & Marks, T. J. J. (2007). High mobility. Air-stable n-type perylene diimide semiconductors. Insight into

materials Design for stability of n-type charge transport. *Journal American Chemical Society*, 129, 15259-15278.

[33] Serap, G., Neugebauer, H., & Sariciftci, N. S. (2007). Conjugated Polymer-based Organic Solar Cell. *Chemical Reviews*, 107, 1324-1338.

[34] Würthner, F., Stepanenko, V., Chen, Z. J., Saha-Moller, C. R., Kocher, N., & Stake, D. J. (2004). Preparation and characterization of regioisomerically pure 1,7-disubstituted Perylene bisimide dyes. *Journal of Organic Chemistry*, 69, 7933-7936.

[35] Ke, D., Tang, A., Zhan, C., & Yao, J. J. (2013). Conformation-variable PDI@ β -Sheet nanohelices show stimulus- responsive supramolecular chirality. *Chemical communication*, 49, 4914-4916.

[36] Clean Solar Energy Guide. (2013). www.konarka.com

[37] Greeg, B. A., & Ferrere, S. (2002). New Perylenes for dye sensitization of TiO₂. *New Journal of Chemistry*, 26, 1155-1160.

[38] Wilson, J. N., GAO, J., & Kool, E. T. (2007). Oligodeoxyfluorosides: strong sequence dependence of fluorescence emission. *New Journal of Chemistry*, 63, 3427-3433.

[39] Meier, H. (2005). Conjugated oligomers with terminal donor acceptor substitution. *Angewandte Chemie International Edition*, 44, 2482e50.

- [40] Kim, C. S., Tinker, L. L., Disalle, B. F., Gomez, V., Lee, S., Bernhard, V., & Loo, V. (2009). Altering the thermodynamics of phase separation in inverted bulk heterojunction organic solar cell. *Advanced Materials*, 21, 3110-3115.
- [41] Jorgensen, M., Norman, V., & Krebs, F. C. (2008). Stability/degradation of polymer solar cells. *Sol. Energy Material Solar Cell*, 92, 686-714.
- [42] Oyamada, T., Maeda, C., Sasabe, H., & Adachi, V. (2003). Efficient electron injection mechanism in organic light-emitting diodes using an ultra thin layer of low-work-function metals. *Journal of Applied. Physics*, 42, L1535-L1538.
- [43] Kim, S.Y., Hong, K., Kim, K., & Lee, J. L. (2008). Increase of quantum efficiency in Organic light emitting diodes with Mg-Al alloy cathode and RhO₂-coated ITO anode electron. *Materials Letter*, 4, 63-66.
- [44] Kim, H., Shin, V., Park, J., & Kim, Y. (2010). Effect of long time annealing and incident light intensity on the performance polymer; fullerene solar cells. *IEEE Transaction Nanotechnology*, 9, 400-406.
- [45] Etzold, F., Howard, I. A., Mauer, R., Meister, M., Kim, T., Lee, K., Baek, N., & Laquai, F. (2011). Ultrafast Exciton dissociation followed by nongeminate charge recombination in PCDTBT: PCBM photovoltaic Blends. *Journal of American Chemical Society*, 133, 9469-9479.
- [46] Kamm, V., Battagliarin, G., Howard, I. A., Pisula, W., Mavrinskiy, A., Li C., Mullen, K., & Laquai, F. (2011). Polythiophene: Perylene diimide solar cell- the

impact of alkyl-substitution on the photovoltaic performance. *Advance Energy materials*, 1, 297-302.

- [47] Icil, H., & Icil, S. (1996). A Thermal and Photostable Reference Probe for Q_f Measurements: Chloroform Soluble Perylene 3,4,9,10-Tetracarboxylic Acid-bis-N, N-Dodecyl Diimide. *Spectroscopy Letters*, 29(7), 1253-1257.
- [48] Turro, N. J., Neckers, D. C., Leermakers, P. A., Seldner, D., & D'Angelo, P. (1965). Interrelations between the Mass Spectrometry and Photochemistry of Organic Molecules. I. Ketene Dimers and Other Small Ring Compounds. *Journal of the American Chemical Society*, 87(18), 4097-4100.
- [49] Weber, G., & Hercules, D. M. (1966). Fluorescence and Phosphorescence Analysis Principles and Applications, Interscience. *Publishers (John Wiley & Sons)*, New York, 217-240.

APPENDIX

Appendix A: Curriculum Vitae

No. 5, Majidadi Close, off Karofi Street,
Jalingo, Taraba State.

Phone No: +2347037107020
E-mail: bbg2015@yahoo.com

ADAMU ABUBAKAR

Date of Birth: 19th June 1983
State of Origin: Taraba State
L.G.A: Jalingo
Nationality: Nigerian
Gender: Male
Marital Status: Single

Schools Attended with Date

2015 – 2016 Eastern Mediterranean University, Famagusta, North Cyprus.
2005 – 2010 Federal University of Technology, Yola
1999 – 2004 Government Science Secondary School, Jalingo
1993 – 1998 Mafindi Primary School, Jalingo

Qualifications

2016 MSc in organic chemistry-photochemistry
2010 B. Tech (Hons) Industrial Chemistry
2004 Senior School Certificate
2006 Senior School Certificate
1998 First School Leaving Certificate

Working Experience

Industrial Attachment

Kaduna Refining and Petro Chemical Company (KRPC),
Product Programming and Quality Control Department

- Responsibilities:
 - Flash Point
 - Viscosity
 - Codrasont Carbon Residue (CCR)
 - Distillation
 - Sulphur Content

National Youth Service Corps (NYSC) 2011

Ag. HOD and Chemistry Teacher, Chemistry Dept, Sama Secondary School,
Argungu, Kebbi State

- Responsibilities:
 - Teaching and Community Development

- Conduct and Supervision of Examination

Laboratory Technologist, Chemistry department, Taraba State University, Jalingo (2012-2014)

Graduate assistant, Chemistry department, Taraba State University, Jalingo (2014 - date)

Hobbies:

Football and Travelling